June 2020

Coastal Taxodium distichum Growth Responses to Marine Influences and Stand Density

Stephanie Moothart
Louisiana State University and Agricultural and Mechanical College

COASTAL TAXODIUM DISTICHUM GROWTH RESPONSES TO MARINE INFLUENCES AND STAND DENSITY

A Thesis

Submitted to the Graduate Faculty of the
Louisiana State University and
Agricultural and Mechanical College
in partial fulfillment of the
requirements for the degree of
Master of Science

in

The School of Renewable Natural Resources

by
Stephanie Marie Moothart
B.S., Colorado State University, 2016
B.A., Colorado State University, 2016
August 2020

ACKNOWLEDGEMENTS

I would like to thank my committee members Drs. Richard Keim, Thomas Dean, Sammy King and John White for your continued advice and feedback. Special thanks to my major advisor Dr. Keim for allowing me to design my project and giving me support along the way. Thank you to the other professors who took the time to assist me including but not limited to Drs. Mike Kaller, Andy Nyman, and Steven Midway.

I would like to thank the Lake Pontchartrain Basin Foundation, particularly Dr. Eva Hillmann and the Louisiana Department of Wildlife and Fisheries, particularly Duck Locascio for helping to collect samples from their sites and providing me with previous data.

Thank you to everyone who helped me with my arduous fieldwork: Alicia McAlhaney, Savannah Morales, Mary Grace Lemon, Cameron Rutt, Alessandra Bresnan, Matt Shockey, and especially Britt Fleming. Thank you graduate students of the School of Renewable Natural Resources for your help and guidance, especially my lab mates from the Keim Forest Ecohydrology Lab, Nga Nguyen, Alicia McAlhaney, Savannah Morales, and Mary Grace Lemon and my office mates C.J. Pell and Antonio Cantu as well as any of the graduate students who gave me advice and encouragement.

Thank you to the friends and family across the country for conversations and reassurances. Thank you to my parents Tom and Karen Moothart for instilling a love of the outdoors young as well as your unending support and encouragement. Thank you to my brother, Josh Moothart for being a listening ear. Thank you Alex Rice for being there for me with encouragement, inspiration, food, distractions and care.

TABLE OF CONTENTS

ABSTRACT

Ecological processes controlling transition areas of coastal wetlands between marshes (not forested) and swamps (forested) are poorly understood, despite important ecosystem services provided and strong interest in managing for ecosystem structure and function. The objective of this work was to identify how soil chemistry and stand density control individual-tree growth of the important coastal species baldcypress (*Taxodium distichum* (L.) Rich.) and pondcypress (*Taxodium distichum* var. *imbricarium* (Nutt.) Croom) along a coastal salinity gradient. Tree cores, soil samples, and stand density measurements were collected for sixty cypress trees at the coastal Joyce Wildlife Management Area, Louisiana, which is a former forested wetland that partially transitioned to marsh following salt-water intrusion in the 20th century. There was strong correlation between tree-ring chronologies and water levels and rainfall as expected. Soil concentrations of sea-water components (S, Na, Mg, Ca) and electrical conductivity of pore water followed the hypothesized geographic gradient across the site of higher values near the source of seawater. Concentrations of these salinity-associated components were higher at 30 cm depth than at the surface, suggesting recent flushing, but concentrations of plant nutrients (P, K, Ca, Mn) were higher at depth, suggesting concentration by plants. Unexpectedly, cypress growth efficiency—basal area increment per sapwood basal area—was not correlated to stand density or soil chemistry. A principal component analysis of tree-level growth sequences indicated that the trees living in higher salinity were proportionally less responsive to high salinity (drought) years as compared to trees further inland. Thus, trees on the forest-marsh edge, which experience the most seawater influence, apparently have some mechanism to compensate for or avoid salinity. The most likely explanation is that microhabitats

such as hummocks might be critical in understanding controls on cypress growth and persistence in marginal sites such as this.

INTRODUCTION

In coastal Louisiana wetlands, there are transition areas from open seawater to marshes (not-forested wetlands) to swamps (forested wetlands). The swamps are mostly cypress-tupelo forests with baldcypress (*Taxodium distichum* (L.) Rich. var. *distichum*) and pondcypress (*Taxodium distichum* var. *imbricarium* (Nutt.) Croom) being the main species. Understanding cypress growth controls is an important component of understanding the ecology of forest-marsh transitions.

Salinity from seawater is one of the most important influences on coastal wetland vegetation composition, and the saline-fresh transition zone often coincides with the swamp-marsh transition zone. Intrusion of seawater into forested wetlands can cause a change in the dominant ecosystem community through mortality of cypress. Cypress is a freshwater species that can tolerate some salinity, depending on the concentration and duration of saturation, but too much salinity over prolonged periods of time causes mortality (Krauss et al. 2009, Shaffer et al. 2009) and even small amounts can reduce growth (Conner and Ozalp 2002, Liu et al. 2017). Hoeppner et al. (2011) found that salinity as low as 1-2 ppt decreases growth of cypress and complete tree mortality can occur at 2-6 ppt, and Krause et al. (2009) found evidence of cypress mortality and reduced stand density at even lower concentrations (0.7 ppt and 1.3 ppt). Day et al. (2013) demonstrated that the variable most highly correlated with tree growth (as shown in tree rings) was salinity, and Thomas et al. (2015) found that effect of growth of mature cypress along the salinity gradient was important, independent of flooding.

Constituents of seawater have individual effects on plants so can be necessary nutrients but in high concentrations they are toxic. Seawater is composed of chloride, sodium, magnesium, and sulfur as the four most prevalent elements (Day et al. 1989). Salinity interferes with tree

metabolism, and responses to these and other specific components of seawater such as sulfur have their own, partially independent, effects on plants, and thus may be dominant factors controlling the separation between swamp and marsh. At high concentrations of sulfate, reduction of sulfur produces toxic hydrogen sulfides, placing stress on cypress that may be the dominant biogeochemical driver of the forest-marsh division (Hackney and Avery 2015). Sulfur becomes bound in organic matter instead of remaining in ionic from as do many components of seawater. Thus, S could persist for longer than sodium and other components, so that plants may be susceptible to S toxicity after seawater intrusion even after salinity has been reduced by flushing. Powell et al. (2016) found that salinity (chloride) and sulfate had different effects from each other saplings in the field and in the greenhouse, but the lowest growth came with high concentrations of both (Powell et al. 2016).

Tree growth rates are the key measure of response to stressors but environmental stressors act in concert with competition stress to control overall growth of individuals. Competition can be inferred from stand density, where denser stands indicate more competition control on individual-tree growth and sparser stands indicate other limiting factors. The effect of competition on tree growth may be affected by salinity. In a meta-analysis of sparse freshwater stands, Allen et al. (2019) found that surviving trees grew better than they did in denser stands; however, salinity effects overwhelmed any density effects on growth rate. This idea was further examined in freshwater systems showing that competition among individual trees was the dominant effect on tree growth over flooding disturbances (McAlhaney 2018).

Cypress growth can be measured by basal area increment (BAI), the growth in basal area over a given time. Another way to measure cypress growth is through growth efficiency (E) which is defined as growth given the resources available to it (carbon dioxide and light) as

quantified by leaf area (Waring et al. 1981). Leaf area is challenging to measure. Because of the relationship between leaf area and sapwood area—the currently active wood transporting water and nutrients—it can be used as a proxy for the crown size (Allen et al. 2015). One way to measure growth efficiency using the sapwood is to measure the annual growth increment (BAI) per sapwood basal area (O'Hara 1988, Dean et al. 1988, Allen et al. 2019). Previous work has shown that E_{sap} can be a useful metric of individual-tree growth sensitivity to both competition and growing conditions of baldcypress (Allen et al. 2019, McAlhaney et al. in press).

Swamp-marsh mechanisms are important to understand because swamps provide important ecosystem services including water filtering, flood and storm protection, and habitats. Cypress can disrupt waves, decreasing their power and protecting shorelines. Cypress-tupelo swamps are also important habitat for a variety of flora and fauna including alligators, birds, snakes, fish, and insects. Disturbances such as natural subsidence dams, levees, canals, dredging, logging, agriculture conversion, sea level rise, and other anthropogenic effects can cause a decline in swamp ecosystem services by transition them into marshes and eventually open water. The transition from forest to marsh can be irreversible, even if the conditions are changed, because the marsh grasses might outcompete any reestablishing cypress seedlings. The changes that lead to wetland loss in the Mississippi River Delta are complex (Day et al. 2000). Not only is salinity intrusion from seawater flooding one of the major drivers of wetland loss (Allen et al. 1996) but it is projected to increase with rising sea level and increased subsidence along the coastal delta in Louisiana.

Ecological restoration of swamps to regain some of the lost ecosystem functions and the services they provide is occurring. Herbivory, nutrient availability, vegetation competition (Myers et al. 1995), flood regimes (Keim et al. 2013a), salinity intrusion, biogeochemical

alteration, land subsidence, and other factors that can lead to degradation. One tool for restoration is reconnecting swamps to the river system. Previous studies have shown that tree growth in swamps hydrologically connected to rivers is greater than in impounded swamps (Day et al. 2012) because increased freshwater, sediment, and nutrients are provided by the river connection. Plantings are occurring in Louisiana as part of restoration efforts and improved understanding of the controls on cypress growth in swamp-marsh transition zones could direct these efforts. More knowledge of the transition zone is necessary for management of cypress swamps in Louisiana.

RESEARCH OBJECTIVES

Broad Objective: This project seeks to examine the controlling process for the divide between marsh and swamp in coastal wetlands.

Research Question: How does cypress growth respond to variable soil chemistry and stand density on a salinity gradient?

METHODS

For this study, 60 sites were selected and sampled from February through May 2019 in the Joyce Wildlife Management Area in Louisiana (Figure 1). All but two sites were accessable by boat only and the ground varied from semi solid to submerged. Soils were mapped by McDaniel (1990) as mostly Maurepas muck (euic, hyperthermic Typic Haplosaprists), with Barbary muck (very-fine, smectitic, nonacid, hyperthermic Typic Hydraquents) in more sediment-rich sites near river channels. At each sample site, a sample tree was cored, stand density was measured around the sample tree, and soil samples were taken to assess growing conditions.

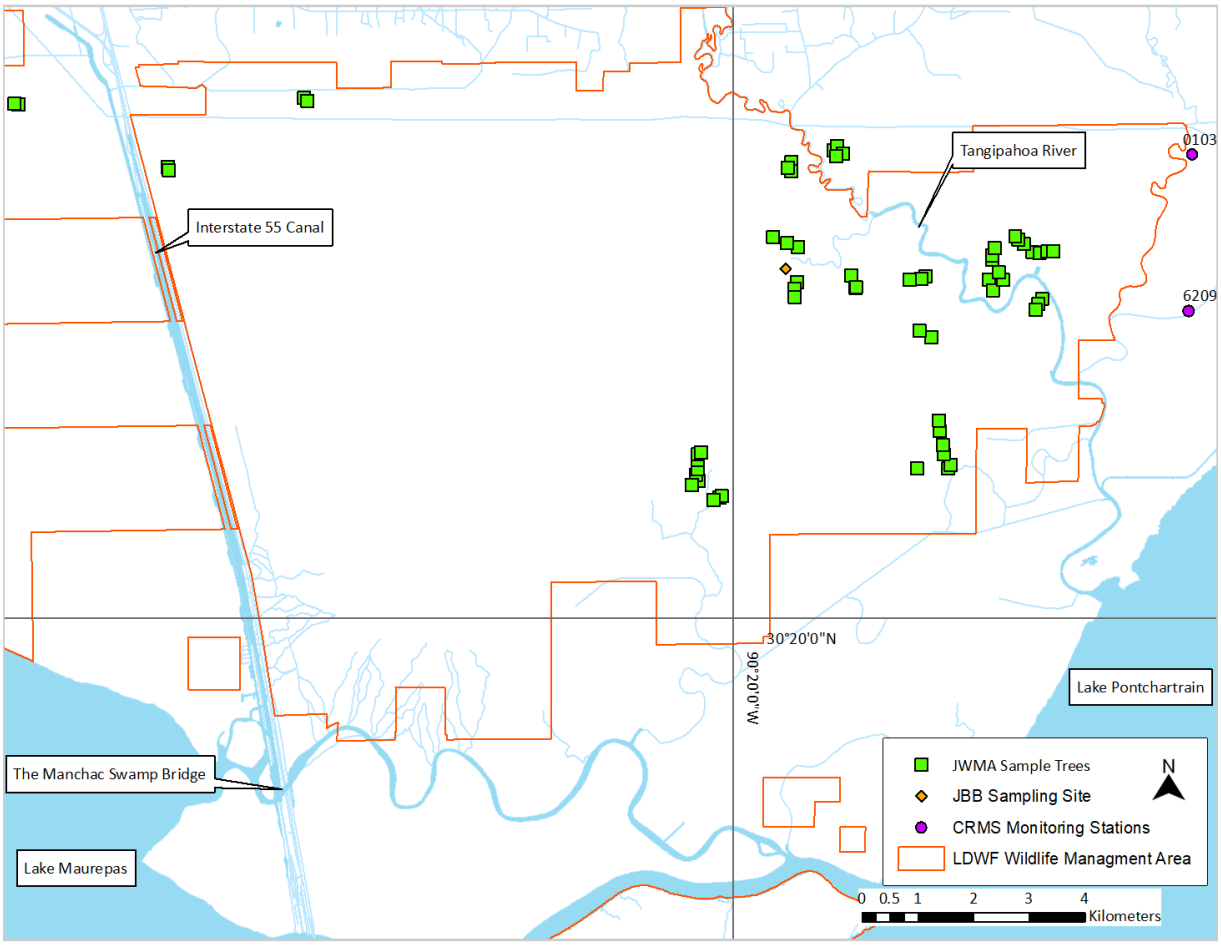

Figure 1. Map of the 60 Joyce Wildlife Management Area (JWMA) sites, 2 Louisiana Coastwide Reference Monitoring System (CRMS) sites, the Joyce Black Bayou (JBB) site and Wildlife Management Areas (LDWF_WMA) outline.

STUDY SITE

The study site is a large, forested swamp situated between lakes Pontchartrain and Maurepas, south of Ponchatoula, Louisiana, and within the Joyce Wildlife Management Area (JWMA). This area has experienced several anthropogenic hydrological changes resulting in subsequent forest degradation in terms of total land area. The leveeing of the Mississippi River in the late 18th and early 19th centuries disconnected the river from its flood plain restricting the influx of fresh water, sediment, and nutrients. In 1968 the Mississippi River Gulf Outlet canal (MRGO), which led straight from the gulf to the adjacent Lake Pontchartrain, was completed and allowed seawater to intrude into the area (Day et al. 2000). This seawater intrusion killed and stressed organisms that were not salt tolerant, including a large mortality rate among baldcypress (Hunter et al. 2016). Some study sites showed up to 100% mature tree mortality in 11 years (Shaffer et al. 2016). Some of these forested swamp areas converted to intermediate-salinity marshes. A total of 610 hectares of cypress swamp in the Pontchartrain Basin was lost as a direct impact of the salinity intrusion and 3,240 hectares of cypress swamp were lost or converted as an indirect result (U.S. Army Corps of Engineers 2012). When the MRGO was closed, in 2009, this source of potential for seawater intrusion was eliminated (Hunter et al. 2016). As a result, wetlands on the margins of Lake Maurepas and Lake Pontchartrain have been getting fresher (Figure 2). There have also been several recent openings of the Bonnet Carré Spillway flood-relief structure on the Mississippi River, which drastically reduces salinity in Lake Pontchartrain for many months (Chao and Yafei 2020). Currently, there are plans to create more openings to reconnect areas around Lake Maurepas with the Mississippi River. We hypothesize that the sea water influx can still be observed in soil chemical concentrations. In addition to hydrologic

changes, the area trees were mined. Removals began in 1885; maximum extraction occurred in the early 1900s with most of the area being cutover by 1943 (Keddy et al. 2007, Norgess 1947).

The study area supports both baldcypress (*Taxodium distichum* (L.) Rich. var. *distichum*) and pondcypress (*Taxodium distichum* var. *imbricarium* (Nutt.) Croom). Other trees in the study site include water tupelo, swamp tupelo, green ash, wax myrtle, red maple, Chinese tallow, and black willow trees. The area in cypress-tupelo is an ecological edge fringing the marsh, varying from dense stands to open canopy (Figure 3).

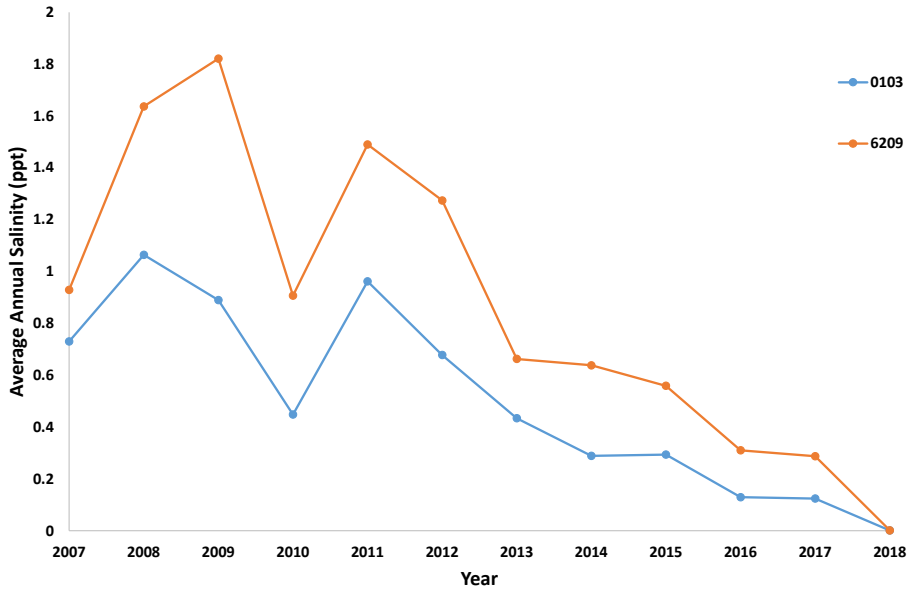

Figure 2. Average annual salinity (ppt) from Coastwide Reference Monitoring System (CRMS) stations 0103 and 6209 near the study area from 2007 to 2018 (Coastal Protection and Restoration Authority (CPRA) of Louisiana 2020).

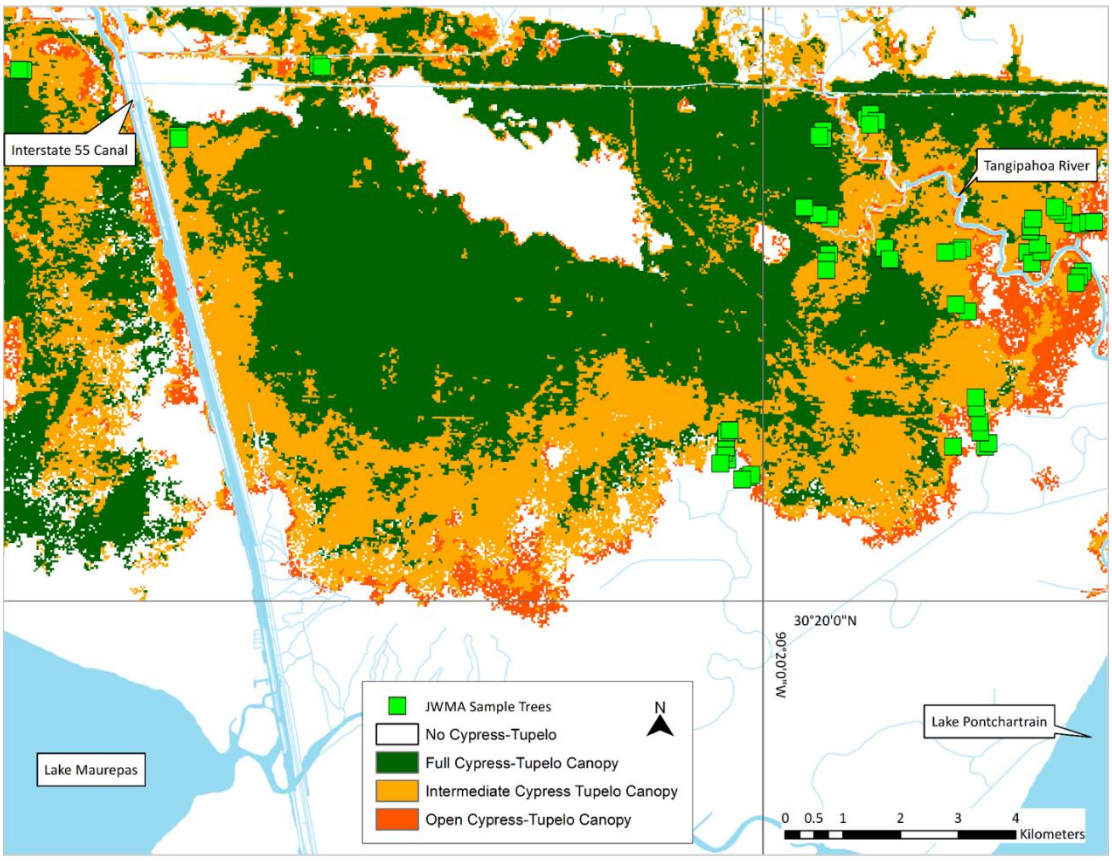

Figure 3. Density of cypress and tupelo trees in the Joyce Wildlife Management Area (Edwards et al. 2019, Keim et al. 2013b).

FIELD SAMPLING

Sampling scheme was designed to capture high and low density plots and high and low salinity plots. Sample trees were always at least 100 meters from each other and were selected based on ease of boat access and position in the forest-marsh transition zone. Sampling occurred February through May of 2019.

120 soil samples were collected; two per site: one from the surface (0-5 cm) and one from a depth of 30 cm (Figure 4). Samples were collected as handfuls of muck, taken from three locations about 2 m from the tree in about 60 degree increments around the tree, and samples were pooled by depth in the field. All soil was removed from above it before the depth sample was taken to best avoid contamination. Temperature-corrected conductivity measurements of soil

pore water were also taken at these three locations at the surface and the 30 cm depth using an electrical conductivity (EC) meter (YSI EC300) to 0.01 µS/cm resolution. All soils were at least saturated—if not ponded—at time of sampling.

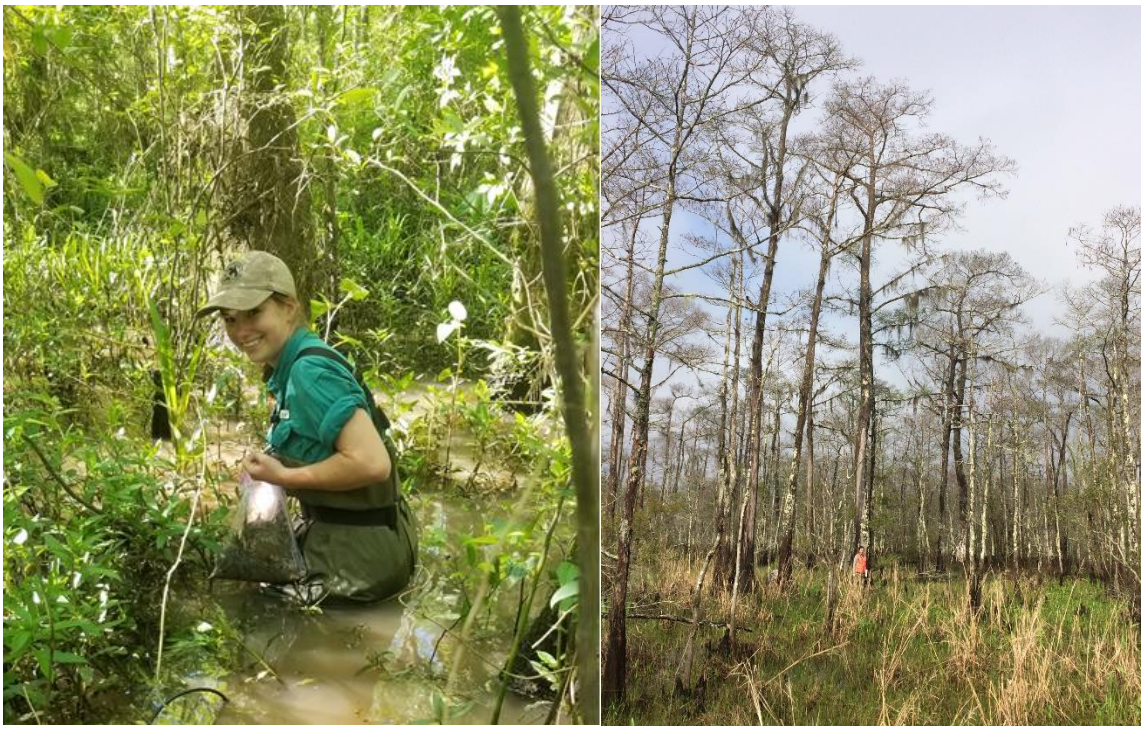

Figure 4. Left: soil collection (from a kneeling position). Right: example of a study site.

All selected trees were *Taxodium distichum* but subspecies var. *distichum* (baldcypress) and var. *imbricarium* (pondcypress) were both represented. The subspecies of each sample tree was not recorded because distinguishing between the two is difficult. The aim of tree selection was to collect across the gradients of both stand density and seawater and to collect a variety of stand densities at each of the seawater gradients. The diameter of each sample tree was measured as normal diameter (46 cm above stem buttressing) to the nearest 0.1 cm using a diameter tape. At least two cores were taken at 90 degree angles around the trunk from the sample tree at the same height as the diameter measurement (generally 1.2-2.5 meters above the ground). The sapwood was identified in the field by coloration and transmission of light through the core from

an artificial light source (Figure 5) (Dean and Long 1986, Vertessy et al. 1995), and sapwood width of the cores was measured in the field using calipers to the nearest 0.01 mm.

Stand density around each sample tree was measured with the sample tree as the center of a variable-radius plot (Grosenbaugh 1952) using 10 BAF and 20 BAF prisms, and the species and diameter of each one as measured by a Wheeler Pentaprism caliper to the nearest 1 cm were recorded. From these data were calculated the trees per hectare and stand density index (Reineke 1933). All trees with diameter < 10 cm were ignored, following McAlhaney et al. (in press), who found that trees with diameters under this were not reflective of the overall stand density and not useful in determining competition pressures on cypress.

Figure 5. Left: measuring the sapwood with a caliper in the field. Right: shining a light through the tree core as confirmation of the line between sapwood and heartwood.

LABORATORY METHODS

All soil samples were refrigerated until they could be dried at 60° C and ground. Subsamples of 2 g were then digested using 20 mL Mehlich 3 acid extractant (Mehlich 1984), and analyzed by inductively coupled plasma mass spectrometry (ICP) for concentrations of P, K, Ca, Mg, Na, S, Cu, and Zn by the Louisiana State University Agricultural Center Soil Testing

and Plant Analysis Laboratory. Subsamples of 10 g were also digested using diethylenetriaminepentaacetic acid (DTPA) (Baker and Amacher 1983) and analyzed by ICP for concentrations of iron, copper, manganese, and zinc at the Louisiana State University Agricultural Center Soil Testing and Plant Analysis Laboratory. All tests were with replicates and laboratory blanks to ensure accuracy. Three undigested subsamples 3 g were weighed before and after (±0.0001 g) ashing in a furnace at 550° C for two hours to estimate the proportion of organic matter as loss on ignition (LOI) (Hoogsteen et al. 2015, Howard and Howard 1990), and results reported as the mean of the three subsamples.

Samples from a subset of 30 sites (60 samples: 30 from the surface and 30 from 30 cm depth) were selected across the range of geographical location and LOI, organic matter content, for additional testing. These dried and ground samples were combusted at 550° C for 4 hours in a muffle furnace. After combustions, ashed samples of 0.3-0.4 g were digested in 100 mL of 6 N HCl, then filtered for P analysis (Andersen 1976) by ascorbic acid automated colorimetry (AQ2 Automated Discrete Analyzer, SEAL Analytical, West Sussex, England) (U.S. EPA 1993). These digested samples were then tested by ICP-OES (Vista MPX , Varian, Palo Alto, CA) for As, Ba, Be, Cd, Co, Cr, Cu, Mn, Na, Ni, Pb, Si, and Zn in the Wetlands and Aquatic Biogeochemistry Lab in the College of the Coast and Environment at Louisiana State University.

Total S was measured as an index for likely sulfide concentrations, assuming most S in solution is in reduced form because these are microtidal wetlands with organic soils. Sulfide is the critical form of S for plant toxicity in wetlands, and due to the permanent inundation sulfides are the likely form of S at depth (Prietzel et al. 1996). However, measuring sulfide concentration in soil solution is difficult. This is because sulfides readily oxidize (Reddy and DeLaune 2008), and because S reduction varies strongly seasonally and spatially within wetlands (DeLaune et al.

2002, Krairapanond et al. 1991, Willis et al. 2011). The Mehlich-3 extracted S concentrations are likely dominated by S in organic form, assuming the S pools are similar to those of a nearby, but saltier, wetland where Krairapanond et al. (1992) found that 80-91% of S is in organic form. Measurements of redox potential in marshes lakeward of our sites suggests S is likely not to be in reduced form near the surface (Willis et al. 2011), but no experimental evidence is available for these forested wetlands.

Additional P data was compiled from CRMS (Louisiana's Coastwide Reference Monitoring System) stations 0173, 0189, 0192, 0209, 0211, 0224, 0225, 0237, 0253, 0261, 0273, 287, 03054, 3166, 3169, 3565, 3617, 4218, 4529, and 4690. These data are in mg/kg obtained by HCl digestion from depths 0-8 cm, 8-16 cm, 16-24 cm, and 24-26 cm. These stations are in marshes dominated by *Spartina alternflora*, *Saggitaria lancifolia*, and *Spartina patens*.

Tree cores were dried at 60° C. They were then mounted and sanded for examination under a microscope (Figure 6). Cores were cross dated (Stokes and Smiley 1968) by matching ring-width patterns. The width of each ring was measured to ±0.001 mm using a Velmex measuring station. The statistical quality of cross dating was analyzed with the program COFECHA (Holmes 1983, Grissino-Mayer 2001). The program ARSTAN (Cook and Holmes 1986) was then utilized to create a site-level chronology and extract tree-level growth sequences, by correcting for autocorrelation and correcting for low-frequency variance using a 20-year cubic smoothing spline retaining 50 percent variance fitted to each tree. The result was ARSTAN-adjusted ring width indices indexed around mean 1 (Cook and Peters 1981). The site chronology was constructed back to 1940 because that is as far back as tree ring widths could be cross-dated reliably, although most trees were at least several decades older and 9 were older than 200 years.

Climate data were collected from National Oceanic and Atmospheric Administration (NOAA) for comparison across the site with the composite chronology, the mean of all the tree chronologies across the site, since climatic conditions can affect growth (Stahle et al. 2019). The mean monthly Palmer Drought Severity Index (PDSI) for April-June 1940 to 2018 and the mean monthly Palmer Hydrologic Drought Index (PHDI) for May-September 1940-2018, and the May mean sea level (MSL) were compiled for comparison in accordance with relationships with cypress tree-ring chronologies found by Bohora (2012) for cypress in on the JWMA sample site (JBB Fig. 1).

For each tree, I calculated the total basal area, summing the ring widths; estimating missing widths near the pith where necessary, assuming circular growth dimensions. Then the difference in basal areas between each year was calculated as annual basal area increment (BAI). BAI was calculated for 7 and 10 year increments as an absolute measure of growth over that time. The slope of BAI was calculated for 5, 7, 10, 15, 20, 25, 30, 35, and 40 year increments to determine if there was directional growth (recovering or declining). I calculated sapwood growth efficiency (E_{sap}) as the annual basal area increment (BAI) per sapwood basal area--a proxy for crown size (Waring et al. 1981, Waring 1983, O'Hara 1988, Dean et al. 1988). Sapwood basal area was estimated as the annular area with outer radius defined as the mean sum of all ring widths for each core (plus estimates of missing widths near the pith, when needed) and an inner radius that was smaller than the outer radius by the mean of the two sapwood width estimates. Two versions of E_{sap} were created: for BAI over 7 and 10 years, also estimated using sums of ring widths.


Figure 6. Left: sanding the tree cores mechanically before hand-sanding. Right: examination of the tree cores under a microscope.

STATISTICAL ANALYSIS

Electrical conductivity (EC) and salinity are related so EC was converted to salinity (psu) for ease of comparison using the measurements of both electrical conductivity (µS cm^{-1}) and temperature (degrees Celsius) (Hill et al. 1986, Lewis and Perkin 1978).

A 10 year moving window sequence of Spearman Rho ranked correlation between each individual tree growth sequence and the full site composite chronology was calculated to identify periods of time when sample tree growth was more or less consistent across the sample area.

Principal component analysis (PCA) was performed on ARSTAN-adjusted, individual tree ring width indices in year space data matrix from 1975 to 2018 in R using package "factoextra." Only the years 1975-2018 were included because (1) this period includes only recent changes in the estuary and does not extend to prior to the MRGO opening, and (2) to include all sampled data and not be forced to omit individual-tree growth sequences that did not extend to prior to 1975. Use of PCA of individual-tree growth sequences is not common in

dendrochronology. Bunn et al. (2005) employed PCA ordination of years (columns) in site-chronology (rows) space data matrix to investigate how growth through time varied in multiple chronologies. However, the use in this study is akin to that used by Chen et al. (2011), who analyzed ranked, single-dimension-ordinated, individual tree-ring series for correlation with precipitation. Here, the loading of each year on each principal component indicates its important in explaining the variance of individual-tree growth sequences, such that the higher-loaded years had the greatest impact on the overall variance in growth rates of the trees. This technique uses established tree-ring analysis techniques to establish the individual tree-ring series, but treats each tree as a separate recorder of the time series of growing conditions instead of collapsing variance among trees to a single annual average growth index as is done when constructing a chronology.

RESULTS

SOILS

The concentrations of elemental constituents of soils followed the hypothesized seawater gradient; there were higher concentrations closer to Lake Pontchartrain, the source of the influx, although with different concentrations at the surface and at 30 cm depth. The points closer to the source of sea influence at Lake Pontchartrain were higher in Na, S, and Mg both at the surface and 30 cm depth (Figures 7, 8, and 9). Concentrations of all three of these seawater components were higher at 30 cm depth then at the surface, while concentrations of organic matter (LOI), Ca, and P were also generally higher closer to Lake Pontchartrain, they were more highly concentrated at the surface than at 30 cm depth (Figures 10, 11, and 12). Concentration of Mn was also higher at the surface than at 30 cm depth, and higher farther from Lake Pontchartrain. There was no discernable pattern for the distribution of K concentration across the sites but it was higher in the surface than at 30 cm depth. Concentrations of Fe followed no discernable trends with by location or depth.

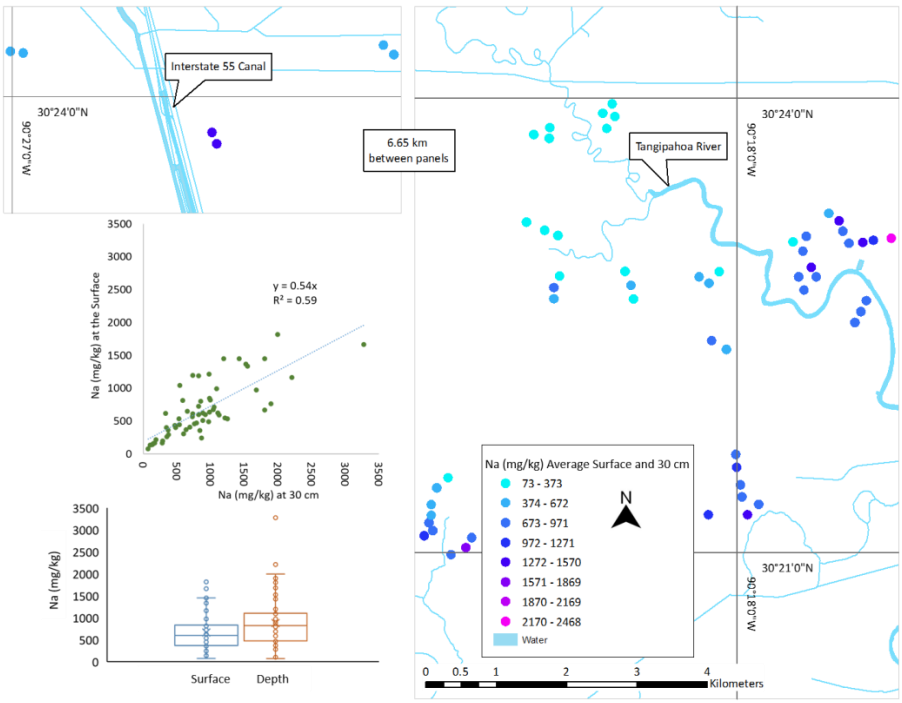

Figure 7. Map of sampling points (locations jittered for visibility), colored by the mean of surface and 30 cm depth concentration of Na (mg/kg). Lake Pontchartrain is to the bottom right of the map. Insets are a boxplot and a scatterplot comparing concentrations at the surface and 30 cm depth; dashed line is a linear regression.

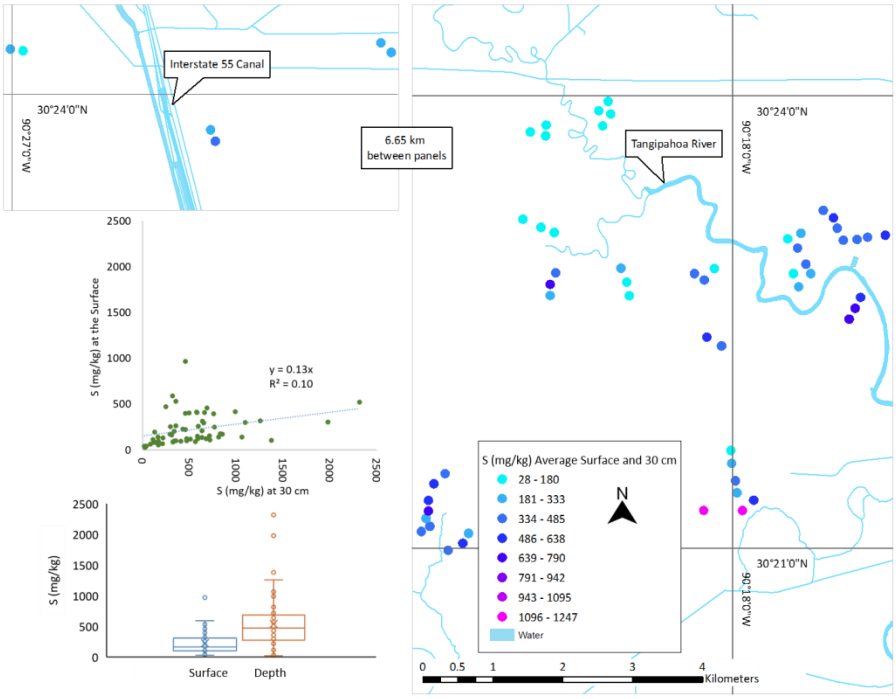

Figure 8. Map of sampling points (locations jittered for visibility), colored by the mean of surface and 30 cm depth concentration of S (mg/kg). Lake Pontchartrain is to the bottom right of the map. Insets are a boxplot and a scatterplot comparing concentrations at the surface and 30 cm depth; dashed line is a linear regression.

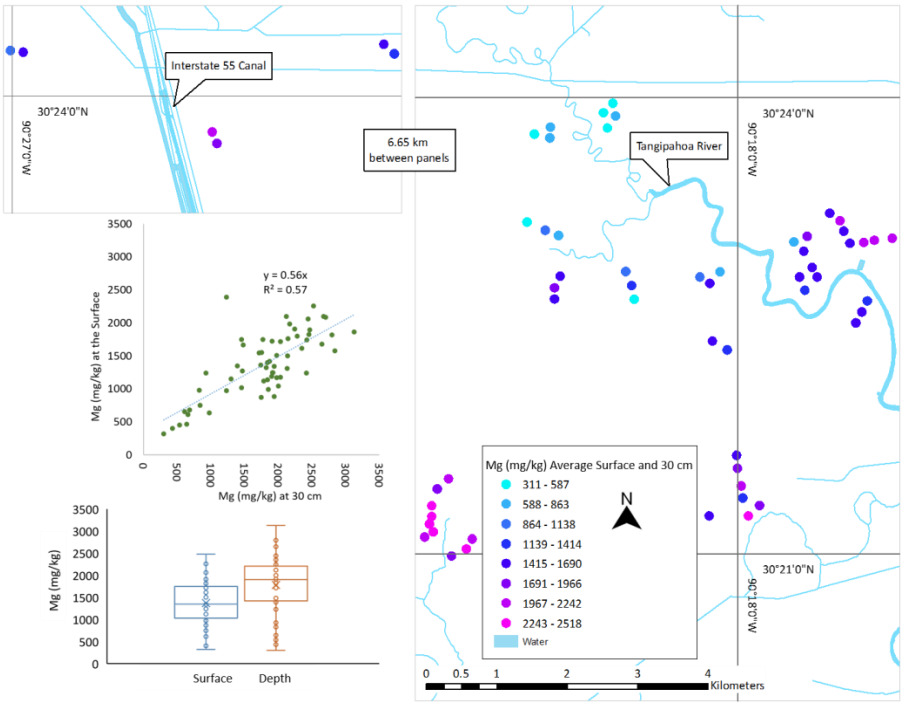

Figure 9. Map of sampling points (locations jittered for visibility), colored by the mean of surface and 30 cm depth concentration of Mg (mg/kg). Lake Pontchartrain is to the bottom right of the map. Insets are a boxplot and a scatterplot comparing concentrations at the surface and 30 cm depth; dashed line is a linear regression.

Electrical conductivity followed spatial and depth patterns similar to S and Na (Figure 10). As a comparison to raw conductivity, the minimum salinity was 0 psu and the maximum was 0.5 psu with a mean of 0.14 psu. This matches nearby CRMS station (0103 and 6209) data (Figure 2) where there was a drop in salinity over the last 10 years. In literature, 0.7 ppt was the highest amount that was discussed as having an effect on stand density and cypress mortality (Krause et al. 2009) which is higher than any value measured in this site.

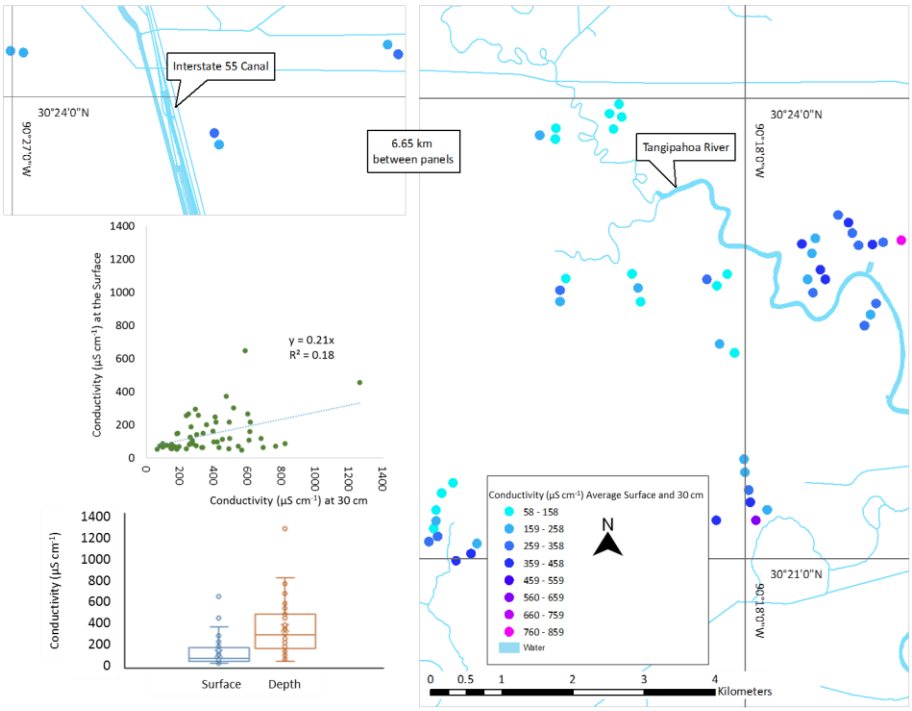

Figure 10. Map of sampling points (locations jittered for visibility), colored by the mean of surface and 30 cm depth concentration of electrical conductivity (µS cm^{-1}). Lake Pontchartrain is to the bottom right of the map. Insets are a boxplot and a scatterplot comparing concentrations at the surface and 30 cm depth; dashed line is a linear regression.

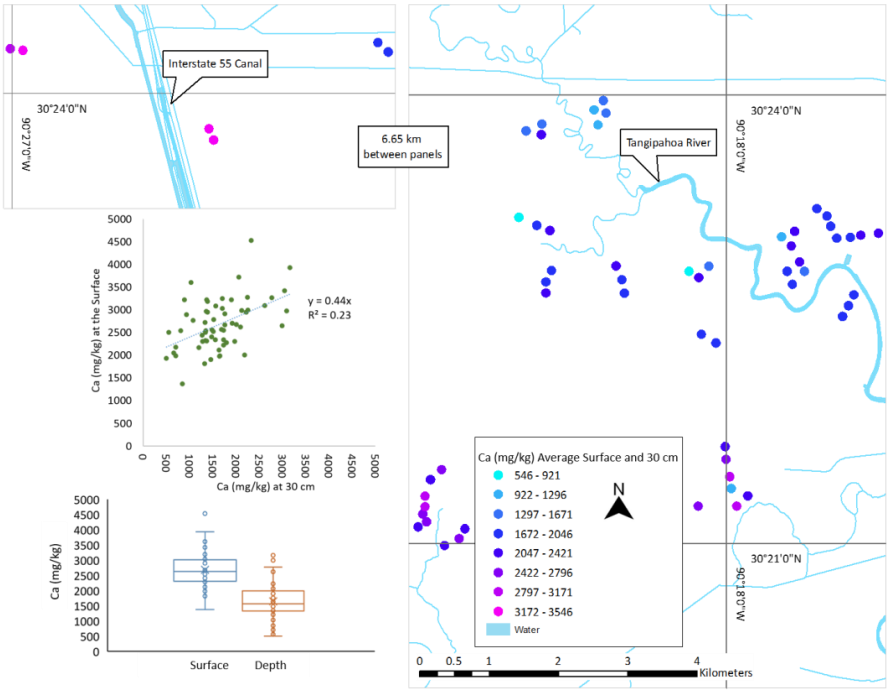

Figure 11. Map of sampling points (locations jittered for visibility), colored by the mean of surface and 30 cm depth concentration of Ca (mg/kg). Lake Pontchartrain is to the bottom right of the map. Insets are a boxplot and a scatterplot comparing concentrations at the surface and 30 cm depth; dashed line is a linear regression.

P concentrations were similar to concentrations collected from CRMS (Louisiana's Coastwide Reference Monitoring System) stations in marshes. The CRMS sites (combining all sites and depths) had a minimum of 105 mg/kg, maximum 4110 mg/kg, and a mean of 815 mg/kg (HCl digestion) compared to the Joyce subsample with a minimum of 378 mg/kg, a maximum of 1240 mg/kg, and a mean of 743 mg/kg (Table 1).

Table 1. Concentration (mg/kg) of each element as extracted by Melich3, DTPA, and digested in HCl from the subset of soils selected for cross-methodological comparison.

	Extractant						Digestion		
	Melich3			DTPA			HCl		
Element	Mean	Min.	Max.	Mean	Min.	Max.	Mean	Min.	Max.
Ca	2000	660	3900	-	-	-	-	-	-
Cu	2.0	0.6	9.2	3.4	1.3	21.0	19.0	11.0	33.0
Mg	1400	460	2700	-	-	-	-	-	-
P	130	21	550	-	-	-	740	380	1200
K	450	88	1700	-	-	-	-	-	-
Na	700	200	1800	-	-	-	1900	520	3500
S	351	87	1097	-	-	-	-	-	-
Z	9.4	2.2	24.0	16.0	3.9	36.0	-	-	-
Fe	-	-	-	400	110	700	-	-	-
Mn	-	-	-	190	14	960	620	31	2600
As	-	-	-	-	-	-	4.8	3.7	6.4
Ba	-	-	-	-	-	-	280	140	540
Be	-	-	-	-	-	-	1.6	0.9	2.5
Cd	-	-	-	-	-	-	4.5	0.4	5.9
Co	-	-	-	-	-	-	14	8.0	31
Cr	-	-	-	-	-	-	64	16	210
Ni	-	-	-	-	-	-	33	12	110
Pb	-	-	-	-	-	-	58	9.6	580
Si	-	-	-	-	-	-	370	220	680
LOI (proportion)	0.69	0.28	0.90	-	-	-	0.70	0.28	0.90

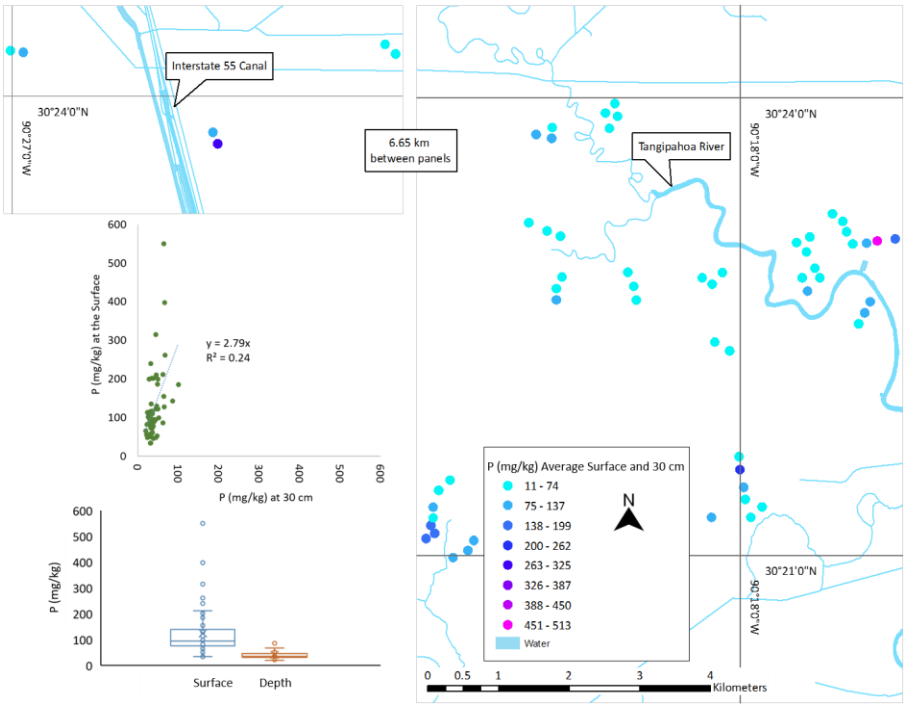

Figure 12. Map of sampling points (locations jittered for visibility), colored by the mean of surface and 30 cm depth concentration of P (mg/kg). Lake Pontchartrain is to the bottom right of the map. Insets are a boxplot and a scatterplot comparing concentrations at the surface and 30 cm depth; dashed line is a linear regression.

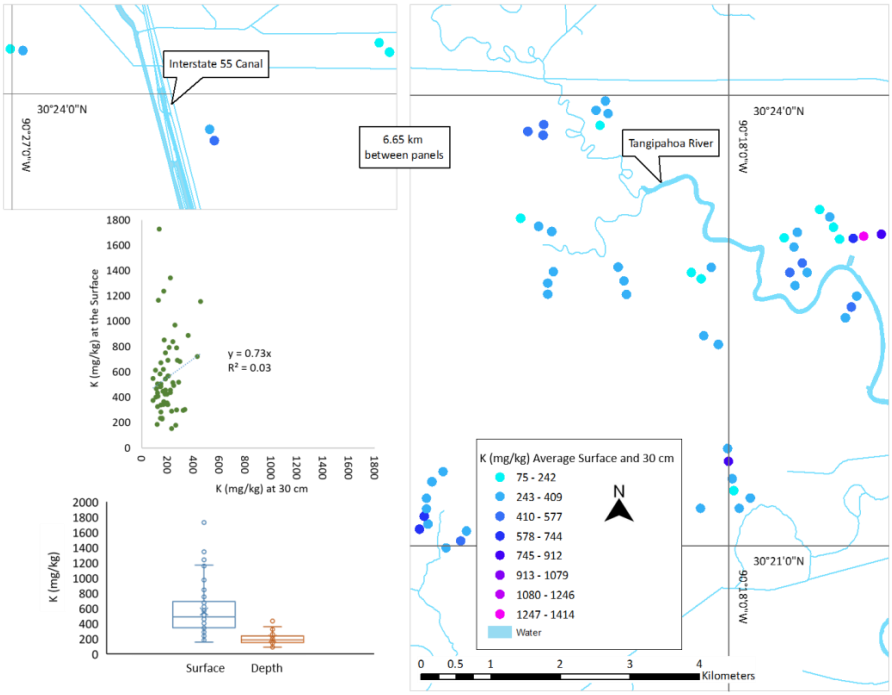

Figure 13. Map of sampling points (locations jittered for visibility), colored by the mean of surface and 30 cm depth concentration of K (mg/kg). Lake Pontchartrain is to the bottom right of the map. Insets are a boxplot and a scatterplot comparing concentrations at the surface and 30 cm depth; dashed line is a linear regression.

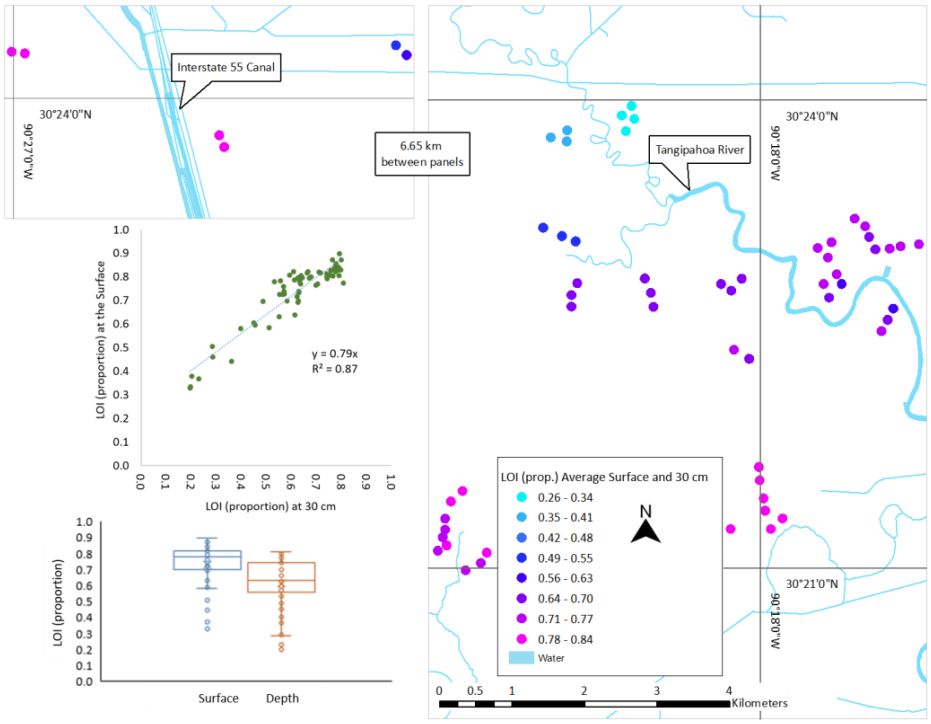

Figure 14. Map of sampling points (locations jittered for visibility), colored by the mean of surface and 30 cm depth loss on ignition (proportion). Lake Pontchartrain is to the bottom right of the map. Insets are a boxplot and a scatterplot comparing concentrations at the surface and 30 cm depth; dashed line is a linear regression.

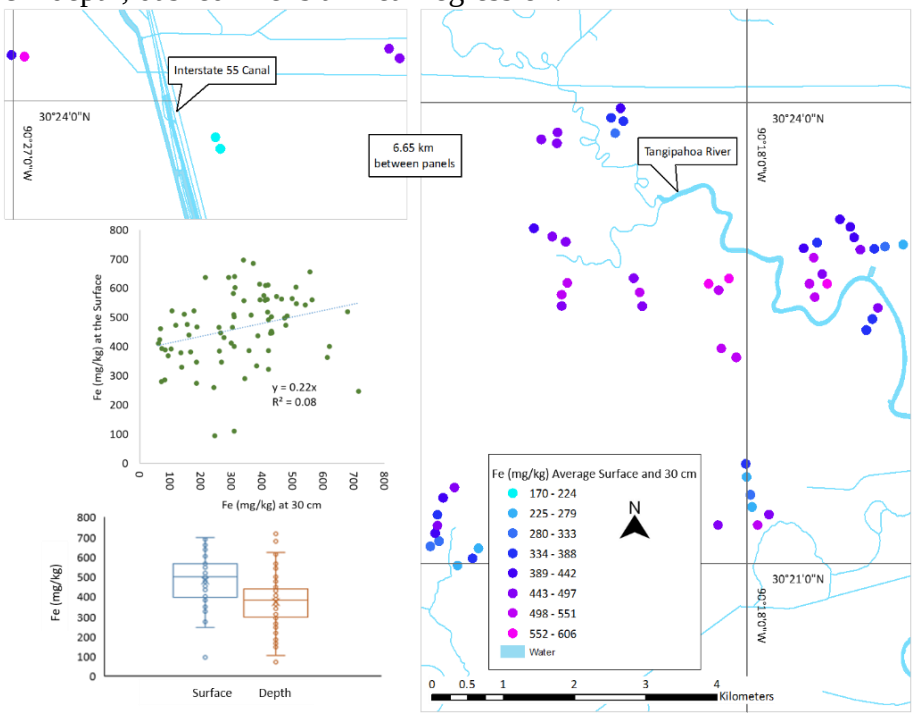

Figure 15. Map of sampling points (locations jittered for visibility), colored by the mean of surface and 30 cm depth concentration of Fe (mg/kg). Lake Pontchartrain is to the bottom right of the map. Insets are a boxplot and a scatterplot comparing concentrations at the surface and 30 cm depth; dashed line is a linear regression.

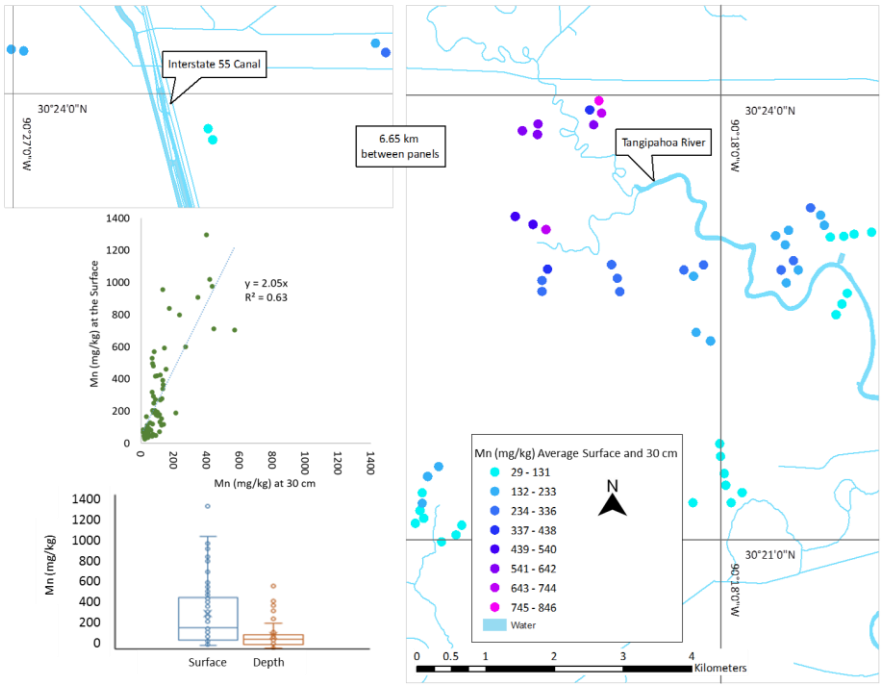

Figure 16. Map of sampling points (locations jittered for visibility), colored by the mean of surface and 30 cm depth concentration of Mn (mg/kg). Lake Pontchartrain is to the bottom right of the map. Insets are a boxplot and a scatterplot comparing concentrations at the surface and 30 cm depth; dashed line is a linear regression.

Correlations among concentrations of soil elemental constituents also mainly followed hypothesized association with sea influence, where concentrations were higher closer to Lake Pontchartrain. Concentrations of elements that are associated with sea water (Mg, Ca, Na, and S) were all positively correlated with each other (Pearson's *r* between 0.41 and 0.82), with electrical conductivity (EC) (*r* between 0.47 and 0.72), and with LOI (*r* between 0.48 and 0.73), reflecting the lakeward gradient toward lower-elevation soils more highly dominated by organic matter and seawater influence (Figure 17). Similarly, LOI was strongly negatively correlated with concentrations of manganese (-0.85) and positively with magnesium (0.74). Manganese was negatively correlated to elements (Figure 17) associated with seawater. The sodium and conductivity where closely correlated (0.84) (Figure 17). Iron was not well correlated to any of the other measured elements (Figure 17). Na and S were highly correlated (0.58) despite recent freshening, suggesting the Na did not flush out more rapidly than did the S.

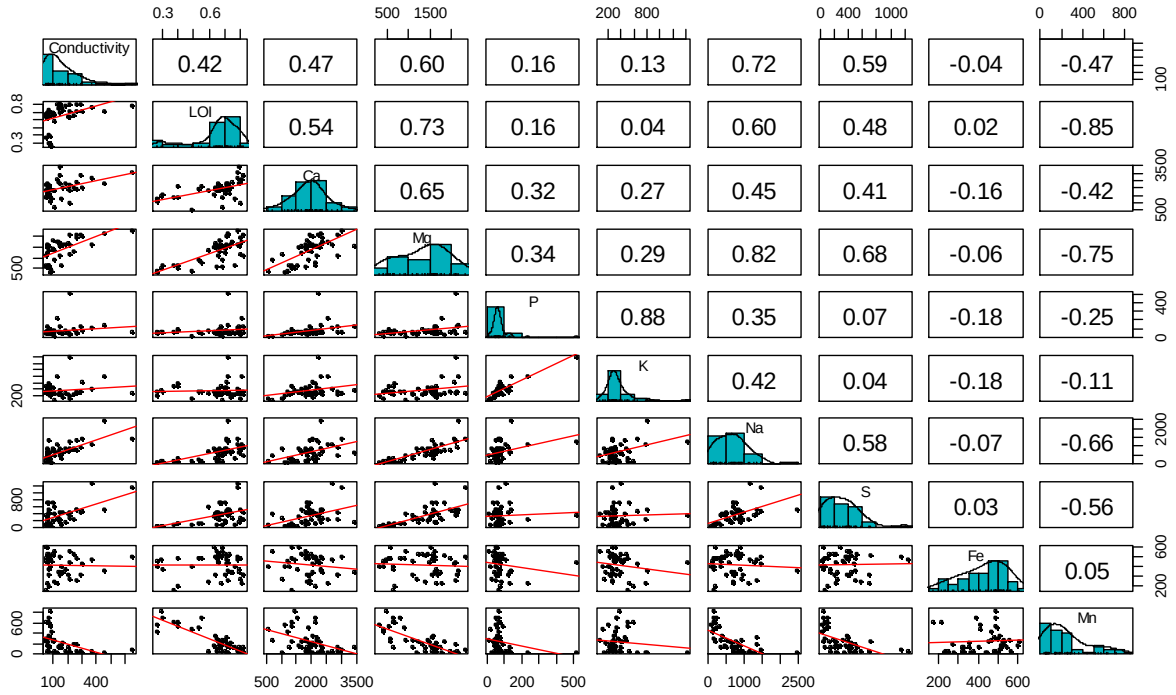

Figure 17. Matrix of the Pearson correlation (top half) and linear regressions (bottom half). Parameters are porewater electrical conductivity (μS cm^{-1}), loss on ignition (LOI, proportion), and elemental concentrations (mg/kg for all), with Ca, Mg, P, K, Na, and S from Melich 3 extractions and Fe and Mn from DTPA extractions.

TREE RINGS

The composite chronology of tree rings was useful, as evidenced by the expressed population signal (EPS) of 0.97 (Wigley et al. 1984). The mean diameter was 36.1 cm. Most trees were at least 80-years old. The oldest tree had rings starting in 1663 with 9 trees over 200 years old and 4 over 300-years old. With an average series inter correlation of 0.392 and a mean sensitivity of 0.357, overall correlation among temporal growth patterns was low. Correlation among individual tree growth chronologies was generally higher during periods of high growth than during periods of low growth (Figure 18). In particular, the high-water years 1977 and 1991 both resulted in high individual growth and high correlations among all temporal tree growth patterns, across time.

Forests grew faster during times with high water and plentiful rainfall the general pattern of tree ring width indices from 1940-2018 matched climate data for the region (r = 0.34) confirming that tree growth is less in drought years at this site (Bohora 2012). The composite chronology was correlated with the average April-June PDSI (*r* = 0.45), the average May-September PHDI (*r* = 0.4), and average May coastal MSL (*r* = 0.32) (Figures 19 and 20).

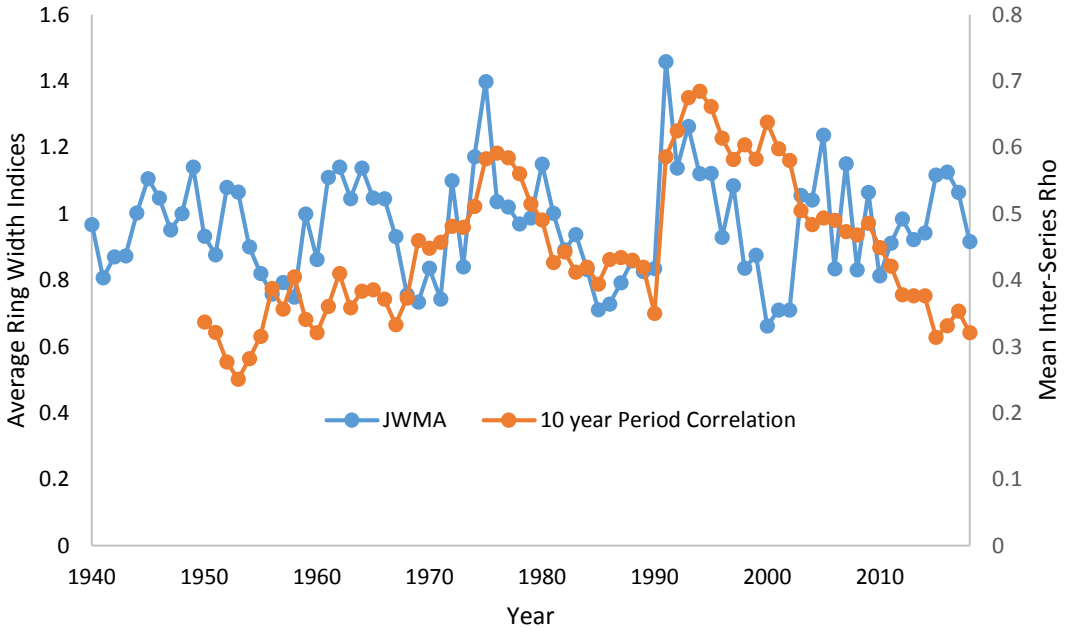

Figure 18. Average inter-series correlation ranked with Spearman's Rho for 10year windows from 1940-2018, where the year corresponds to the period end, compared to the average ring width indices growth of each year from 1940-2018.

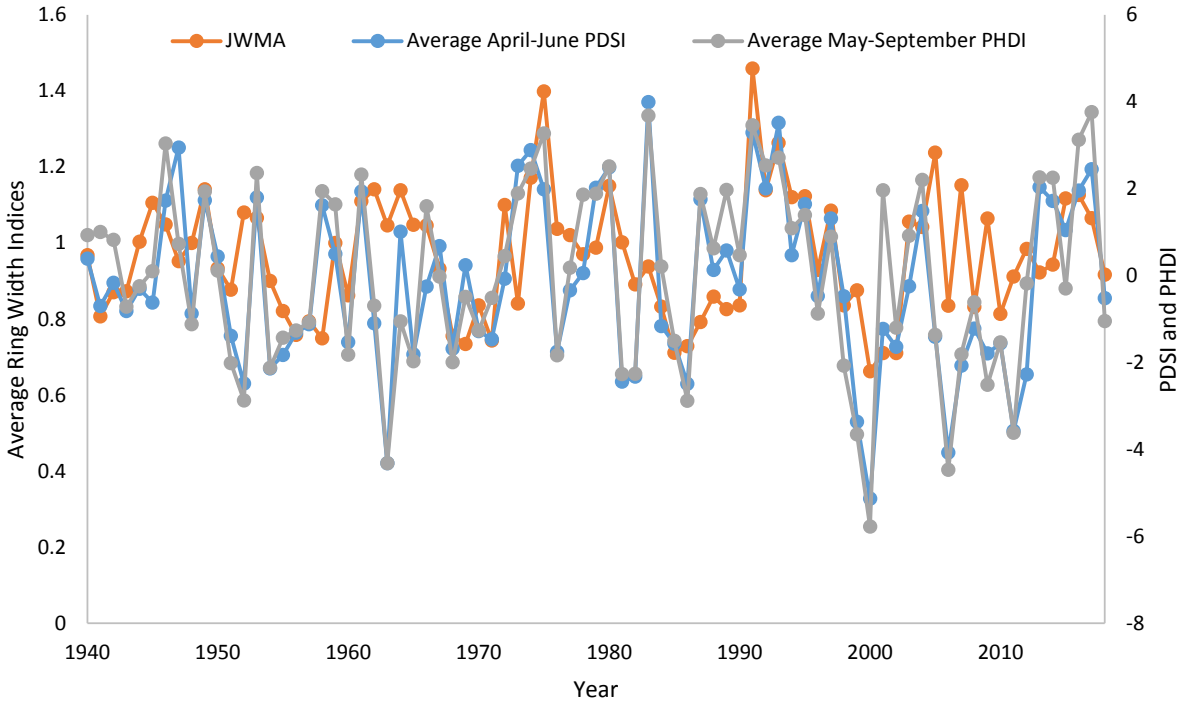

Figure 19. The average tree ring width indices compared to the mean April-June Palmer Drought Severity Index (PDSI) and the average from May-September Palmer Hydrologic Drought Index (PHDI).

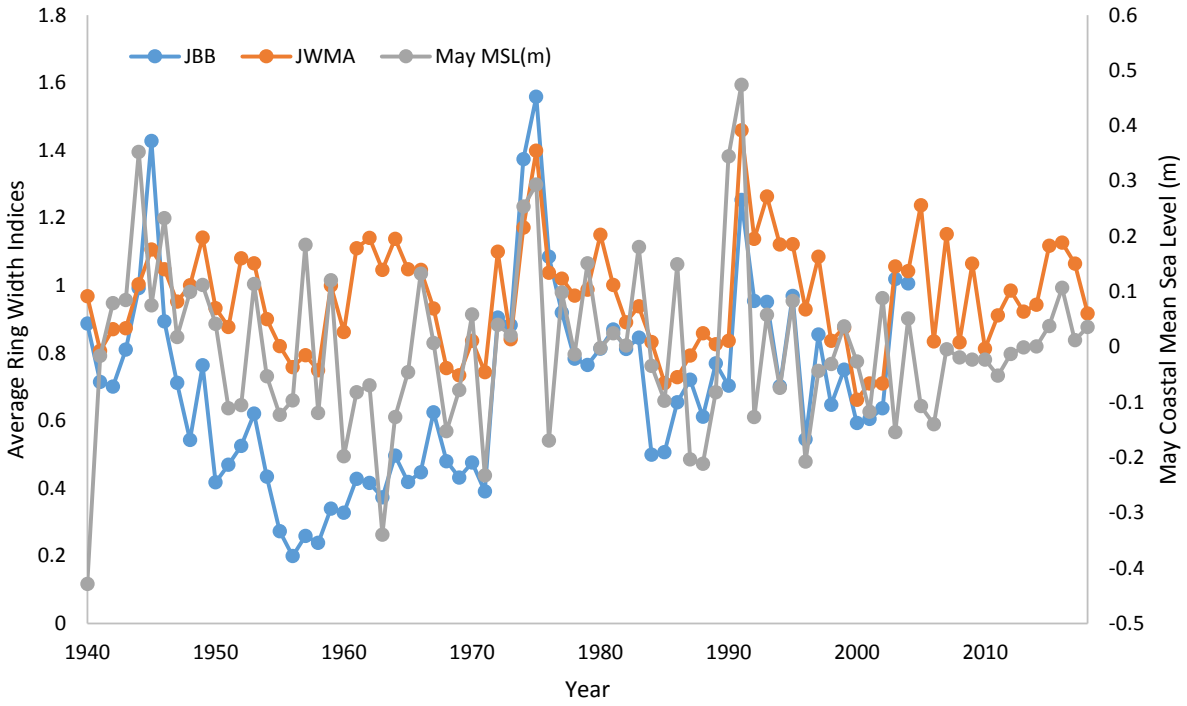

Figure 20. The average tree ring width indices for Joyce Wildlife Management Area (JWMA) and Joyce Black Bayou (JBB) compared to the May coastal mean sea level (MSL) from the National Oceanic and Atmospheric Administration (NOAA) station.

Tree Growth Relative to Stand Density

Overall E_{sap7} was lower and more variable at this study site than it was for cypress trees in the nearby, freshwater Atchafalaya Basin (McAlhaney et al. in press). There was no overall relationship between E_{sap7} and stand density (Figure 21), but there was considerable heteroscedasticity, whereby trees growing near the least-dense situations grew with both the highest and lowest E_{sap7} of all trees in the study and this had the most variability.

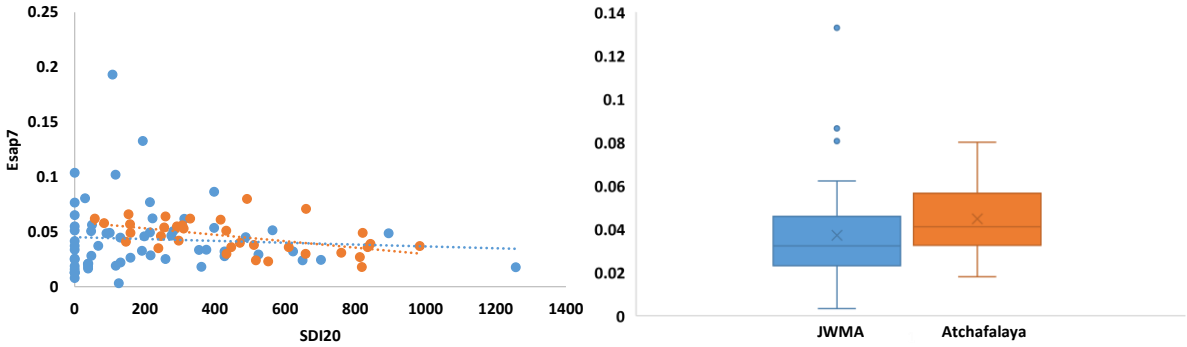

Figure 21. Comparison of E_{sap7} for cypress trees in the Joyce WMA (JWMA) and in the Atchafalaya Basin (McAlhaney et al., in press) with stand density (SDI20).

Despite the intent to sample evenly across the study area, stand density (as measured by stand density index from variable plot cruise with a 20 BAF prism, SDI20) was weakly positively correlated with the diameter of the sampled cypress (r = 0.17) because trees near the margins of the forest were generally smaller and stands there were generally less dense (Figures 22 and 23). Similarly, there were correlations among soil properties and stand density that followed north-south trends in soils pertaining to seawater influence and organic matter content as measured by LOI (Table 2). Stand density index as measured by the BAF10 prism (SDI10) was similar to SDI20 (Figure 22).

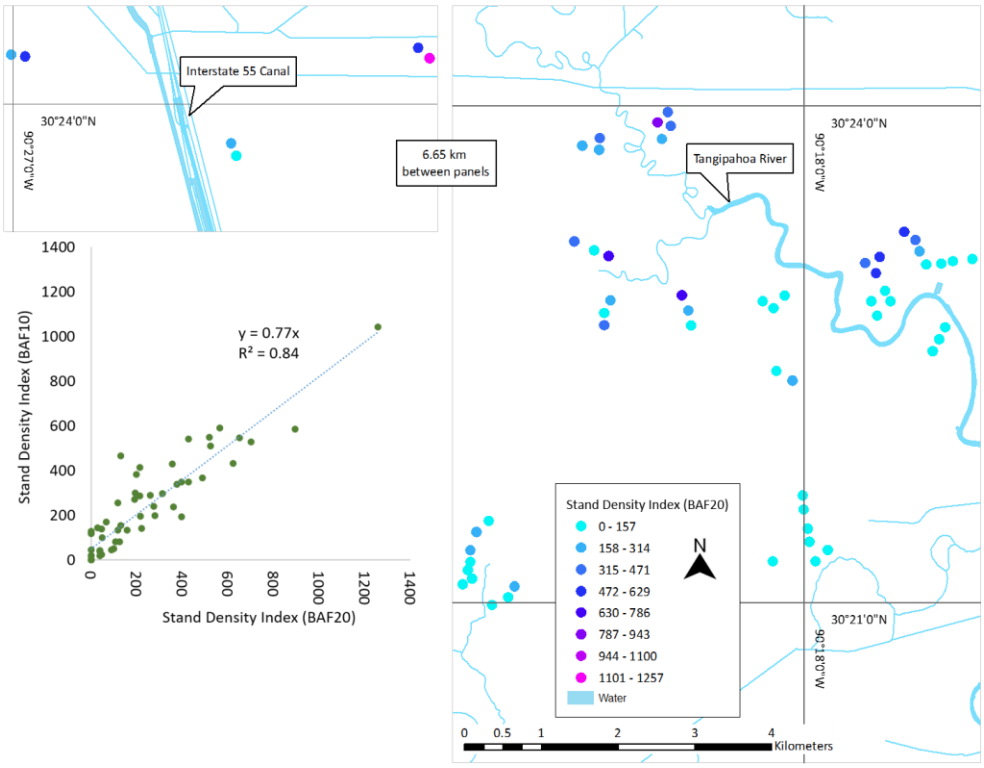

Figure 22. Stand density at study trees (locations jittered for visibility); dashed line is a linear regression. Lake Pontchartrain is to the bottom right of the map.

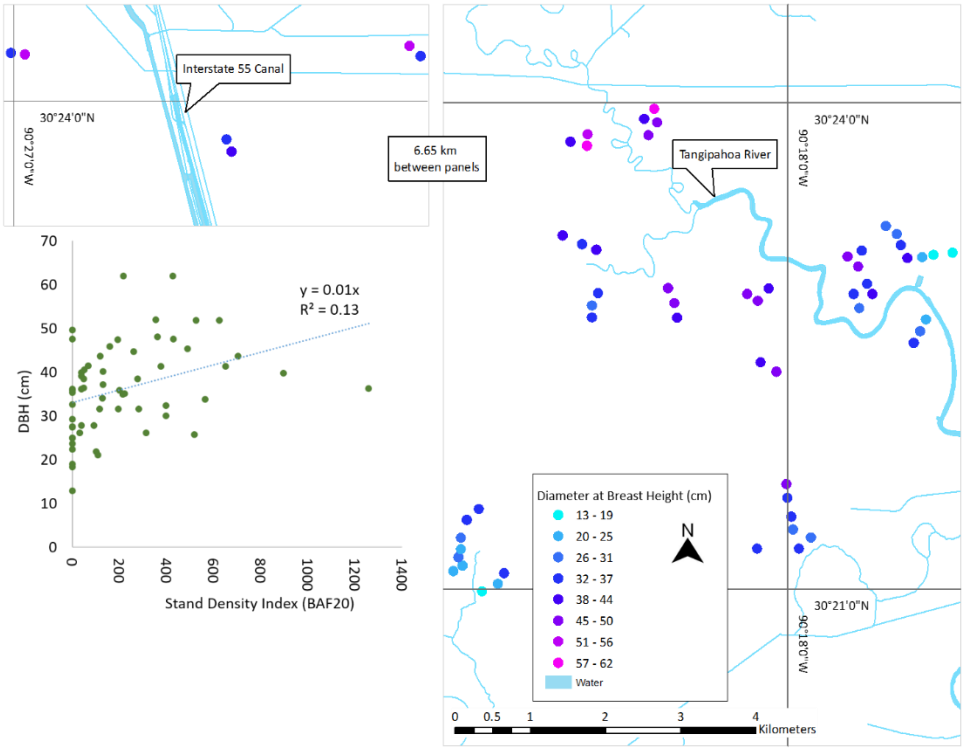

Figure 23. Diameter of study trees (locations jittered for visibility) and inset scatterplot correlation with stand density index; dashed line is a linear regression. Lake Pontchartrain is to the bottom right of the map

Table 2. Correlations (*r*) between measures of stand density (basal area, tree per ha, and SDI; both calculated either from BAF 10 or BAF prim data) soil properties.

Density	Conductivity ($\mu s\ cm^{-1}$)	LOI (proportion)	Ca (mg/kg)	Mg (mg/kg)	P (mg/kg)	K (mg/kg)	Na (mg/kg)	S (mg/kg)
BA10	-0.37	-0.42	-0.16	-0.37	-0.33	-0.34	-0.43	-0.42
BA20	-0.33	-0.06	0.03	-0.09	-0.3	-0.37	-0.34	-0.24
TPH10	-0.33	-0.06	0.03	-0.09	-0.3	-0.37	-0.34	-0.24
TPH20	-0.27	-0.05	0.03	-0.05	-0.23	-0.31	-0.29	-0.2
SDI10	-0.36	-0.37	-0.13	-0.33	-0.31	-0.33	-0.42	-0.38
SDI20	-0.31	-0.37	-0.12	-0.3	-0.26	-0.26	-0.39	-0.34

Tree Growth Relative to Soil Conditions

There was no strong correlation between basal area increment (BAI) and stand density or between BAI and any of the soil chemical concentrations (Appendix; Table D2). There was also no strong patterns in the slopes of any of the BAI year groups (5, 7, 10, 15, 20, 25, 30, 35, and 40) so the cypress across the site are not recovering or declining in a noticeable pattern for any of these year increments (Appendix; Table D2).

There was no strong correlation between growth efficiency, E_{sap}, and stand density (Figure 24). Even accounting for Na concentrations, there was no clear pattern. While trees growing in stands of the lowest stand density also typically grew in stands at low density (despite attempts to sample high-density stands at higher Na concentrations), there were some efficiently growing trees in soils with high Na (Figure 24). S concentrations were not correlated with growth efficiency.

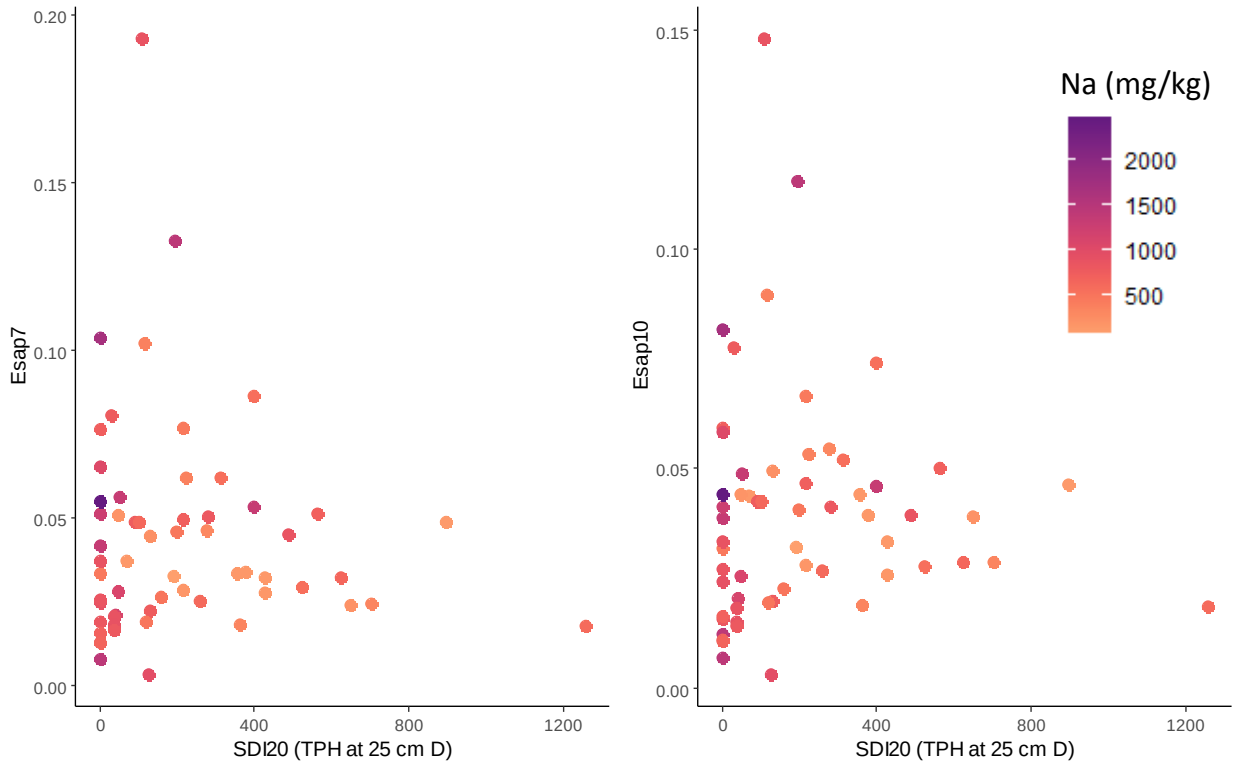

Figure 24. Sapwood efficiency based on 7-year ($E_{sap}7$) and 10-year ($E_{sap}10$) compared to stand density (SDI20), colored by the mean of surface and 30 cm depth soil.

Sapwood efficiency was not generally correlated with soil properties (Figure 25). However, there were two spatial patterns in the growth efficiency measurements (Figures 26 and 27). Within the subset of tress along the Tangipahoa River, E_{sap7} was correlated as expected, where lower-growth trees were closer to the source of the seawater influx on the edge of the forest while the higher growth trees further away. Away from the river, this gradient no longer held and there were some trees with high growth efficiency even though they were on the edge of the forest with high salinity. While similar, the sapwood efficiency for 7 years is more accurate for the stand average because there is an anomalously high year 9 for one tree that alters the sapwood for 10-years (Figures 26 and 27 inset boxplot and scatterplot). There were no strong correlations between the soil characteristics and E_{sap7} (Figure 25). The lack of relationships was not because of confounding by stand density (Figure 25).

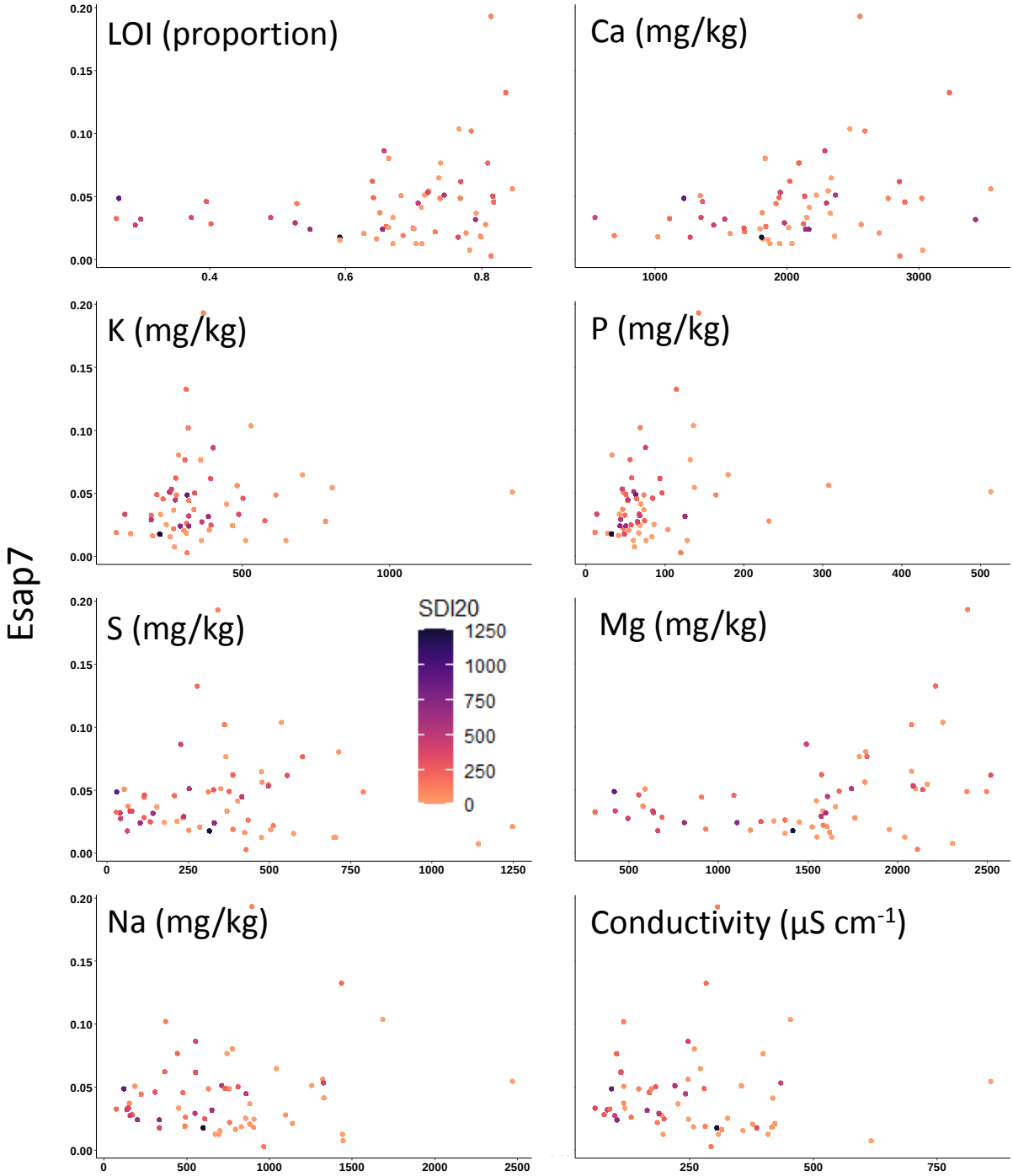

Figure 25. $E_{sap}7$ correlated with soil properties (x-axis) and stand density (coloration) for all trees.

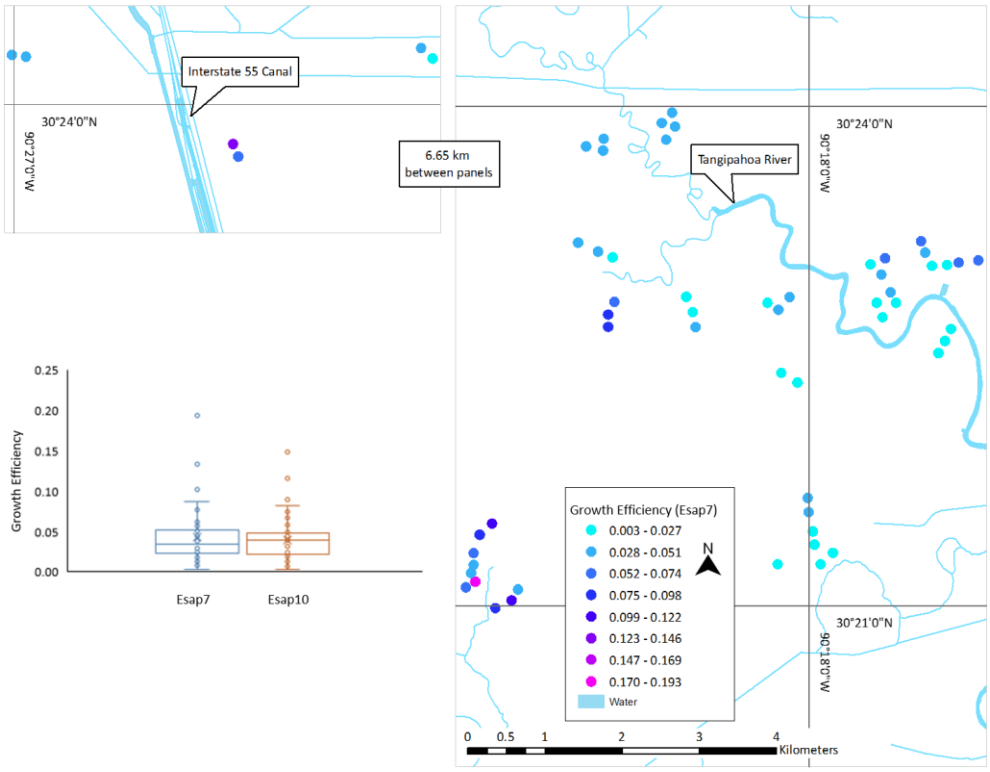

Figure 26. Map of sampling points (locations jittered for visibility), colored by $E_{sap}7$. Lake Pontchartrain is to the bottom right of the map. Inset is a boxplot comparing $E_{sap}7$ and $E_{sap}10$.

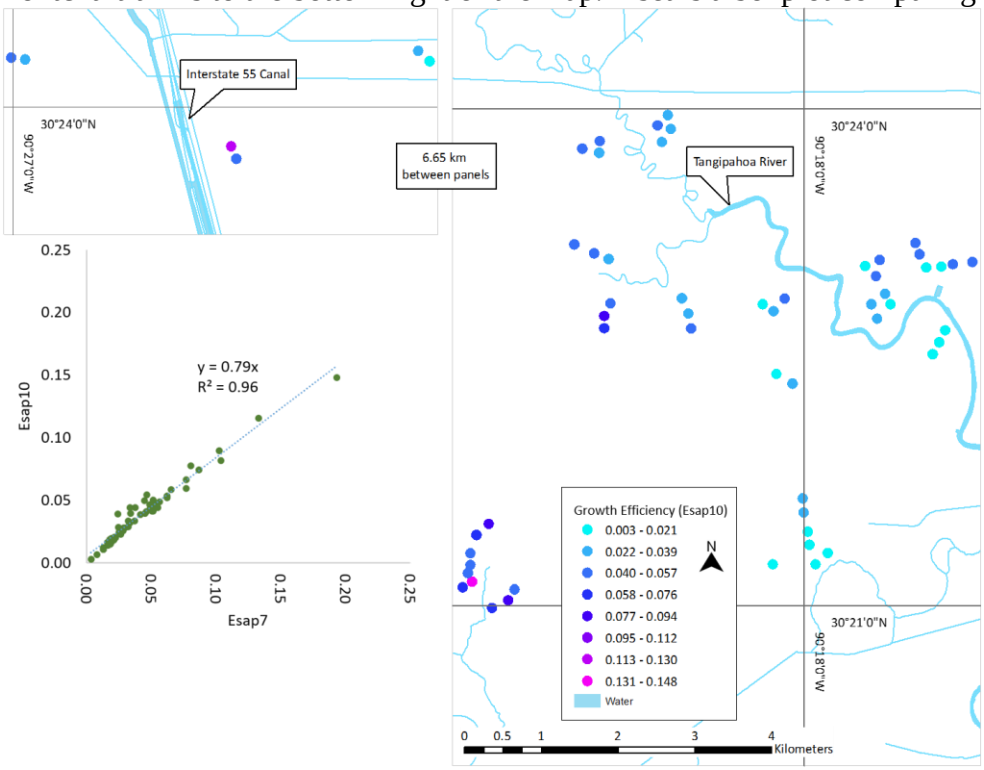

Figure 27. Map of sampling points (locations jittered for visibility), colored by $E_{sap}10$. Lake Pontchartrain is to the bottom right of the map. Inset is a scatterplot comparing $E_{sap}7$ and $E_{sap}10$; dashed line is a linear regression.

Despite lack of correlation between E_{sap7} and soils at the site level, the expected pattern of negative correlation between E_{sap7} and seawater components was weakly evident if only the trees along the river are included (about two thirds of the data) (Figure 28).

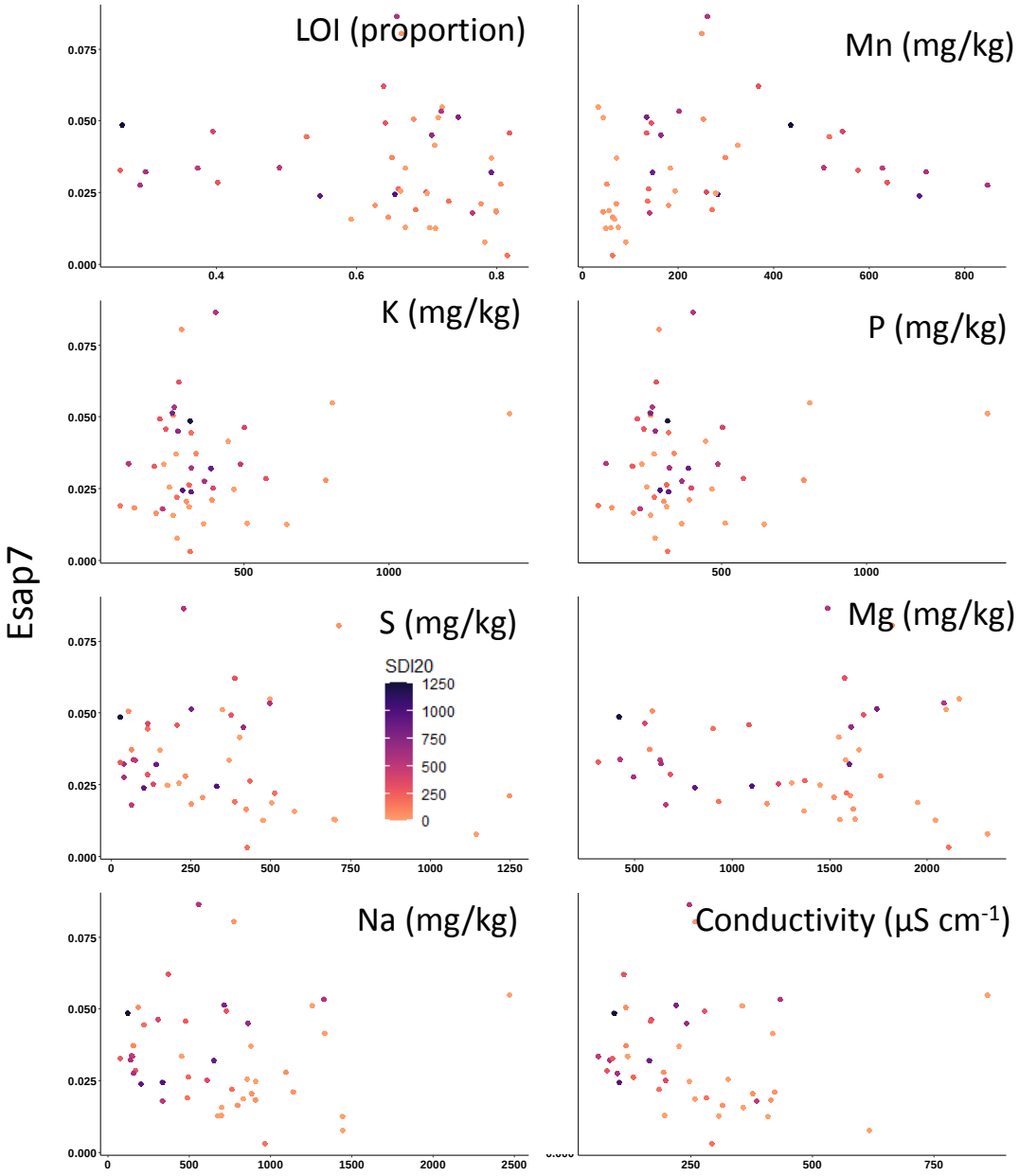

Figure 28. E_{sap7} correlated with soil properties (x-axis) and stand density (coloration) for trees along the Tangipahoa River only.

The principal component of ARSTAN-adjusted individual tree growth sequences in year space data matrix was dominated by a single component (Figure 29). The loading of years on this component (i.e. the years that were most influential for defining differences among individual tree growth chronologies) varied by time and thus environmental conditions (Figure 30). Dry years loaded stronger than did wet years, and years prior to 1981 loaded weaker (Figure 30). For example, the high-water years 1977 and 1991 that were responsible for increasing coherence among trees (Figure 20) were loaded weakly, meaning that tree growth during those years (which was generally high) were not useful for delineating differences among individual tree growth chronologies. Instead, years of drought such as 1988, 2000, and 2011 were most responsible for among-tree growth differences. These years can also be interpreted as likely high-salinity years, given the positive relationship between drought and saltwater intrusion in the Lake Pontchartrain estuary.

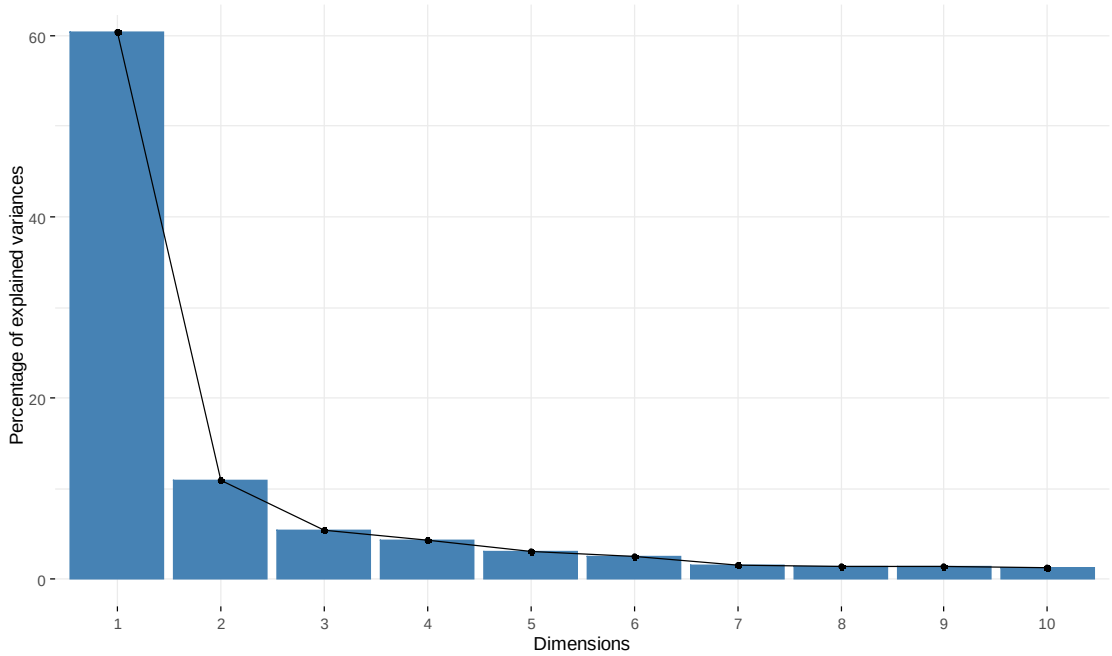

Figure 29. Scree plot of the PCA of ring width indices in year space data matrix comparing the dimensions (years) with the percentage of explained variance in tree ring width indices.

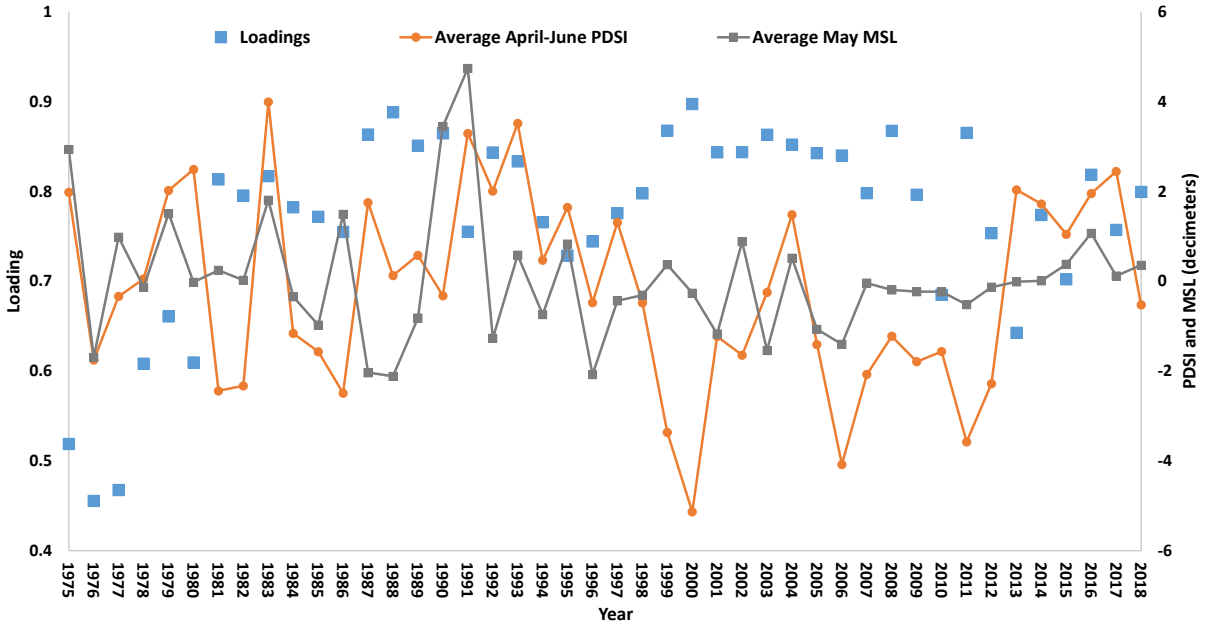

Figure 30. Loadings of years on the first principal component with the mean April-June PDSI and mean May-September PHDI.

There were interpretable patterns in space and in tree-growth relationships to soil conditions in terms of the scores for each tree on the first principal component. This score is highest for trees where the tree growth variance was strongly affected by the highest loaded (dry and salty) years. The lower tree scores (i.e., least sensitivity to dry and salty years) were generally down river and closer to Lake Pontchartrain (Figure 31). The tree principal component score was correlated negatively to the seawater components of the surrounding soil, indicating that the higher the seawater components the less the tree level growth sequence was defined by the highest-loaded (drought) years. Site characteristics affiliated with the lakeward gradient were similarly related to this structuring of tree temporal growth patterns (Table 3). This is similar to the downriver gradient in E_{sap7}; Figure 31 but throughout the site instead of only along the river. Stand density (i.e., competition) played little role in these relationships (Figure 32).

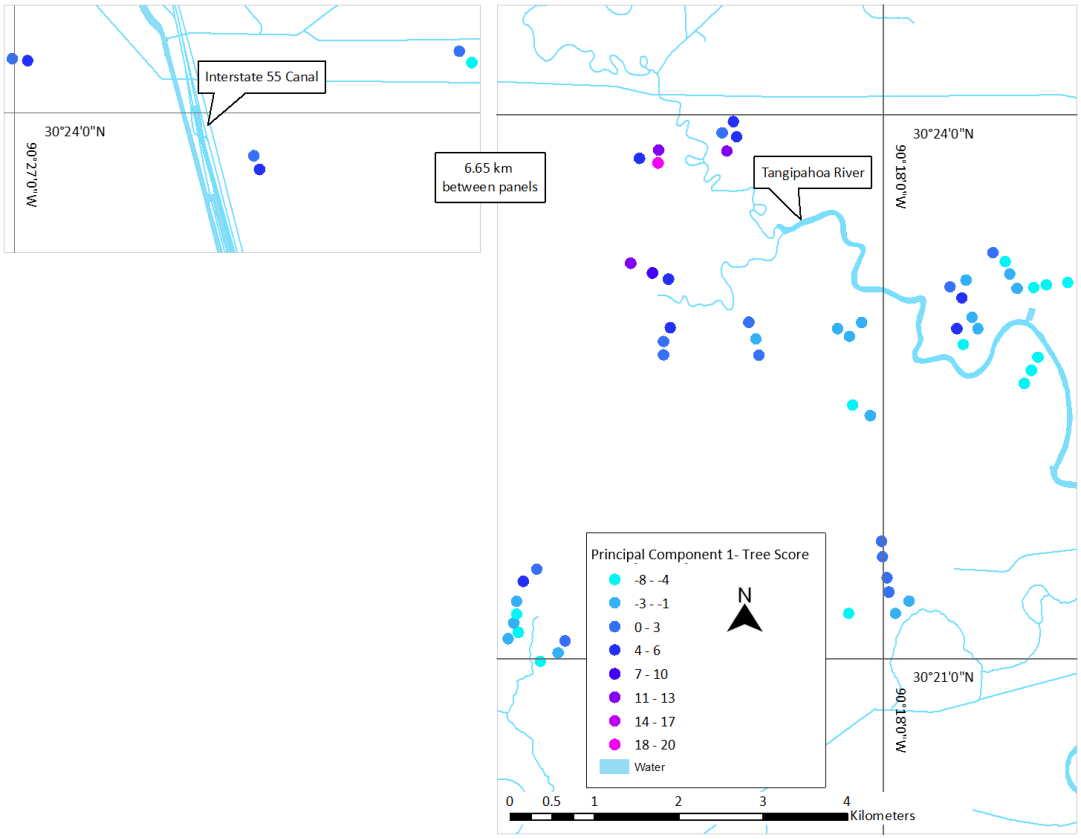

Figure 31. Map of sampling points (locations jittered for visibility), colored by tree score. Lake Pontchartrain is to the bottom right of the map.

Table 3. Correlation (*r*) between the tree principal component score and site characteristics.

Characteristic	Correlation with Tree Score
DBH (cm)	0.67
SDI (BAF20)	0.25
Conductivity (µS cm^{-1})	-0.25
LOI (%)	-0.50
Ca (mg/kg)	-0.18
Mg (mg/kg)	-0.57
P (mg/kg)	-0.16
K (mg/kg)	-0.13
Na (mg/kg)	-0.50
S (mg/kg)	-0.51
Fe (mg/kg)	0.11
Mn (mg/kg)	0.48

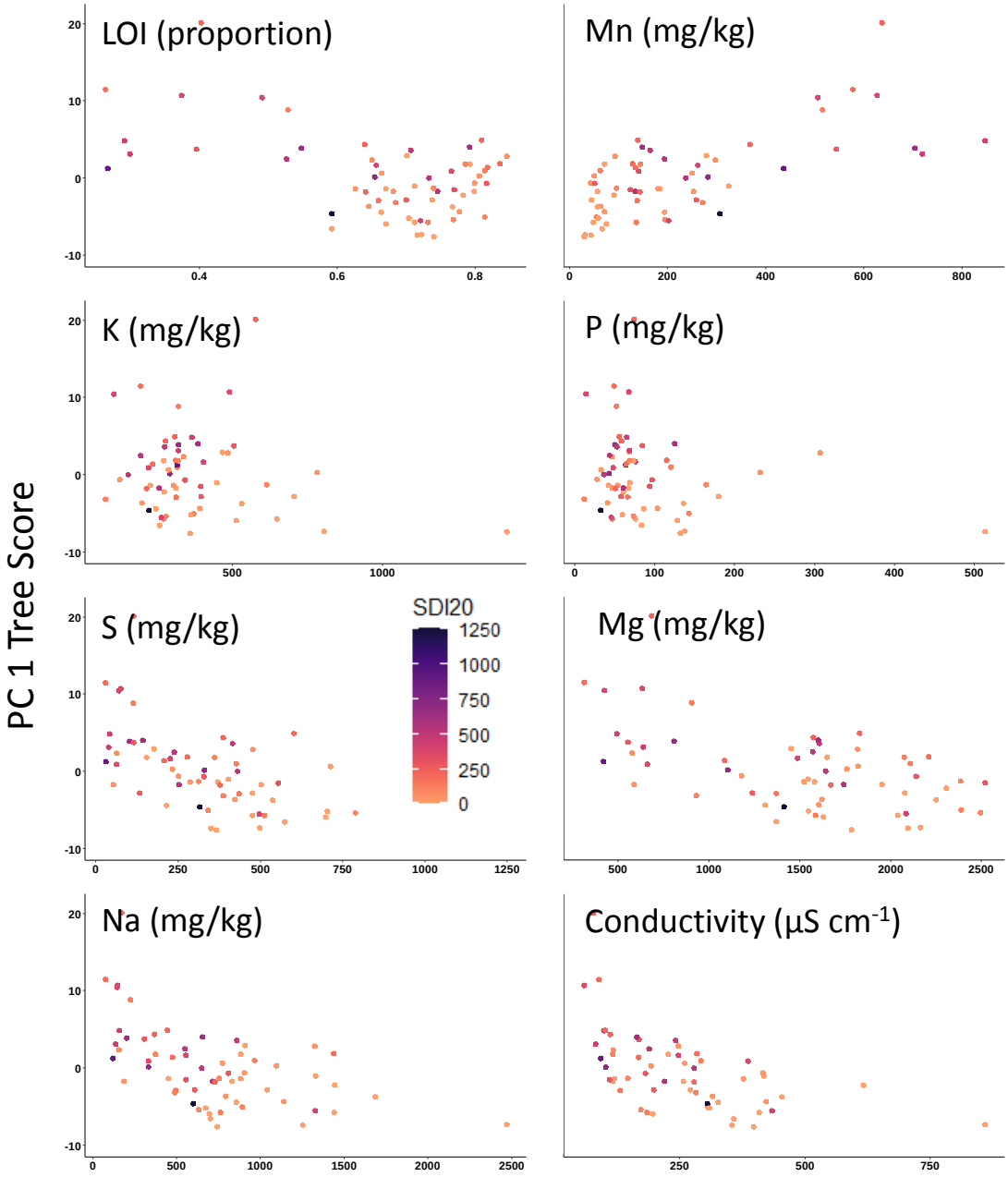

Figure 32. PC1 tree score correlated with soil properties and stand density for all trees.

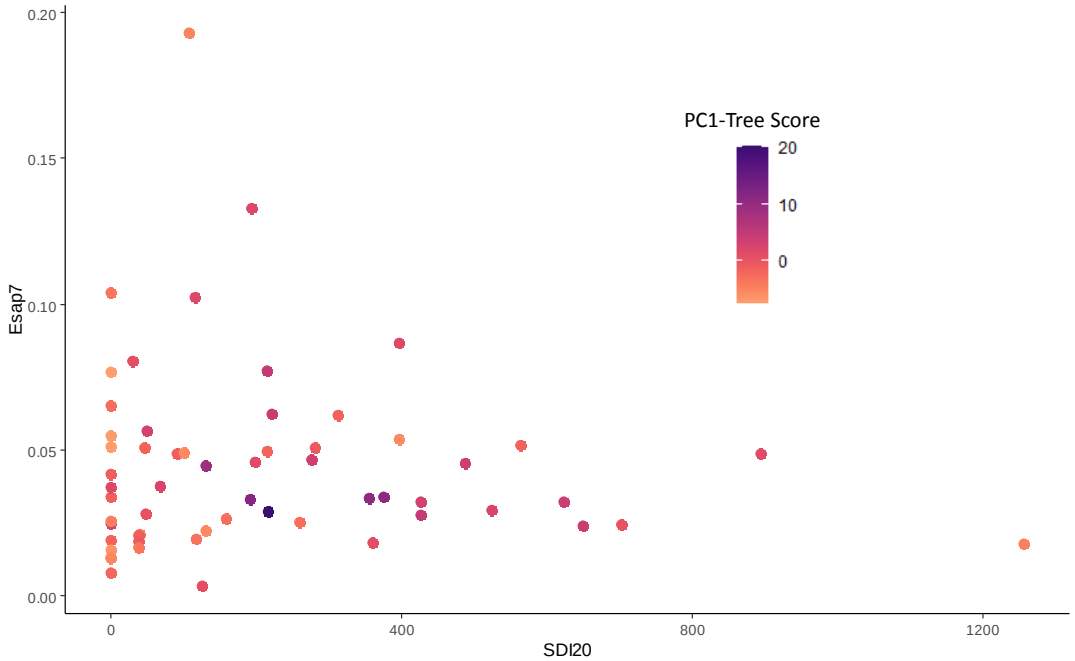

Figure 33. Comparison of E_{sap7} and stand density (SDI20) colored by PC 1 tree score.

DISCUSSION

The hypothesis that conductivity, Na, S, and Mg would be higher closer to Lake Pontchartrain, where the historical influx occurred, was confirmed. However, the tree growth responses at Joyce Wildlife Management Area to marine influence and stand density revealed two apparent paradoxes: (1) cypress BAI and growth efficiency, E_{sap}, was not correlated as expected to known stressors (competition and soil chemistry); and (2) despite the forest-marsh edge being clearly structured by salinity, as reflected in overall stand density, trees on the edge of the transition zone were less sensitive to historical drought and salinity events. While soil chemistry varied geographically across the site in a predictable pattern of historical seawater intrusion, it did not apparently affect tree E_{sap}: neither Na nor S concentrations were correlated to E_{sap} values. The principal component analysis showed that historical drought events that likely led to increases in salinity (Wang et al. 2020) had less effect on trees on the edge that are apparently more exposed to salinity stresses.

There are several possible explanations for these paradoxes. First, trees on the edge of the forest-marsh transition might be taking advantage of microhabitats, either by happenstance or morphological modifications. There is microhabitat variation in the elevation and associated soil chemistry and other stressors across this wetland, as is common in wetlands (Diamond et al. in review). It is possible that the surviving cypress trees along the edge happened to be the ones growing in these slightly advantageous locations that allowed them to survive by evading salinity. Similar results were found in a nearby marginal cypress-marsh wetland where Hsueh et al. (2016) reported isotopic measurements supporting a conclusion that trees preferentially draw on water from hummock tops, above hypoxia and salinity below. Similarly, cypress might have taken advantage of the microhabitats by utilizing morphological plasticity to avoid soil stressors

by preferentially increasing root density in advantageous soil microhabitats. For example, at the surface, salinity and S are lower and S is likely not in reduced form as frequently (Willis et al. 2011, Hackney and Avery 2015). The low amplitude of water fluctuations in this micro-tidal, coastal location with organic soil would likely allow shallow roots to mostly avoid drought and take advantage of higher nutrient concentrations higher in the soil column. If roots are advantageously occupying certain areas, the soil sampling may not have been representative of the soils actually utilized by the roots. Positive correlations between tree ring indices and inter-series correlation support this idea, although the use of high growth years as markers contradicts traditional cross dating methods (Speer 2012). When the trees are growing well, they are doing well across the site, but that when there are poor growth (drought) years they are not poor growth years for all trees; so drought years differentiate trees according to favorable microhabitat.

The lack of relationship between stand density and cypress growth efficiency could also be the result of microhabitats and the nature of competition there. Root competition in microsites such as hummock tops is likely intense, and so root competition might have had a larger effect on tree growth than did the measured tree density. Thus, stand density as measured around sample trees might not have correlated with the tree growth efficiency because the soil microhabitat controls overwhelmed the effect of stand density. The lack of relationship of stand density and growth efficiency conflicts with the hypothesis of Allen et al. (2019) that stand density is positively correlated with individual tree growth because salinity stressors are more intense than is competition. Due to the dominance of the chosen sample trees it is also possible that the trees showed little effect of stand density because the dominant tree is exerting the pressure onto the surrounding stand instead of experiencing it.

Another possible reason for the lack of correlation between known stressors and tree growth efficiency could be genetic differences in the trees. The Joyce Swamp is unusual in that baldcypress (*Taxodium distichum* L. (Rich.) var. *distichum*) and pondcypress (*T. distichum* var. *imbricarium* (Nutt.) Croom) co-occur, and they do so without an apparent spatial pattern. Typically these species are strongly separated by habitat: riverine and deltaic sites are occupied by baldcypress and depressional wetlands are occupied by pondcypress. Similarly, both water tupelo (*Nyssa aquatica* L.) and swamp tupelo (*N. biflora* Walter) rarely occur together in Louisiana but are both present in the Joyce Swamp. Baldcypress and pondcypress are closely related. There is high genetic variation within the subspecies, especially among baldcypress (Lickey and Walker 2002). There is strong evidence of a genetic basis to variability in salinity tolerance (Allen et al. 1997; Krauss et al 2000) but advantages of those adaptations are expressed only in the context of a complex set of environmental conditions (Krauss et al 2009). Liu et al. (1990) found that genetics played no apparent role in survival of baldcypress in thermally altered sites. While genetics might explain some part of the paradox, it is unlikely to be the dominant control because the growth of cypress along the river follow the demonstrated seawater gradient. Thus the paradox only exists away from the river indicating a more site specific control than genetic.

The future of cypress-tupelo swamps in Louisiana is uncertain and there are a number of complex, site--specific factors. Impoundment, seawater intrusion, subsidence, and multiple other factors influence sustainability of the forest (Keim and Amos 2012, Shaffer et al. 2016, Shaffer et al. 2009). Despite these factors, the potential morphological plasticity of the Joyce Swamp cypress indicates it is possible for the mature cypress trees to persist under current conditions. Due to unusually high organic content, the Joyce Swamp also has the potential for organic

accretion to offset subsidence and sea level rise, as has been observed in marshes (Kirwan et al. 2016, Nyman et al. 2006). The salinity was overall quite low (0-0.5 psu), indicating flushing from historical influx levels is occurring, improving conditions for cypress. In an area where most of the dominant sample trees appear to have been established at least 80 years ago, regeneration is a concern. Reforestation plantings have been implemented in the Joyce Swamp (Hillmann et al. 2020) to attempt to offset the lack of natural regeneration. Extrapolations from mature cypress to saplings about morphological plasticity might not be possible as the saplings might not have the same capacity. However, the importance of microhabitats in the success of cypress growth could be important in directing reforestation efforts for site selection. Even construction of mounds for plantings as a microhabitat could be considered though there are complications that require investigation; including the increased weight increasing subsidence, oxidation of organic soils and the effect it might actually have on sapling growth.

CONCLUSIONS

Cypress growth efficiency across a swamp-marsh transition area did not directly respond to a known seawater gradient or to stand density variations. In this organic swamp, concentrations of seawater components were higher at 30 cm depth and concentrations of plant nutrients were higher at the surface. Cypress in areas with the highest concentrations of seawater were least affected by historical salinity increases. These apparently have some mechanism to compensate for or avoid salinity. The most likely explanation is that microhabitats such as hummocks might be critical in understanding controls on cypress growth and persistence in marginal sites such as this.

APPENDIX A. LPBF SAPLING PLANTINGS

The Lake Pontchartrain Basin Foundation has participated in baldcypress tree plantings near the Joyce Wildlife Management Area (Figure A1) to attempt to reforest areas without any mature trees. Soil samples were collected from twelve forest restoration sites where growth is being monitored (Hillmann et al. 2020). The sites have saplings ranging in age from 4 to 6 years old and growth is measured with height and diameter of the trees was taken every year.

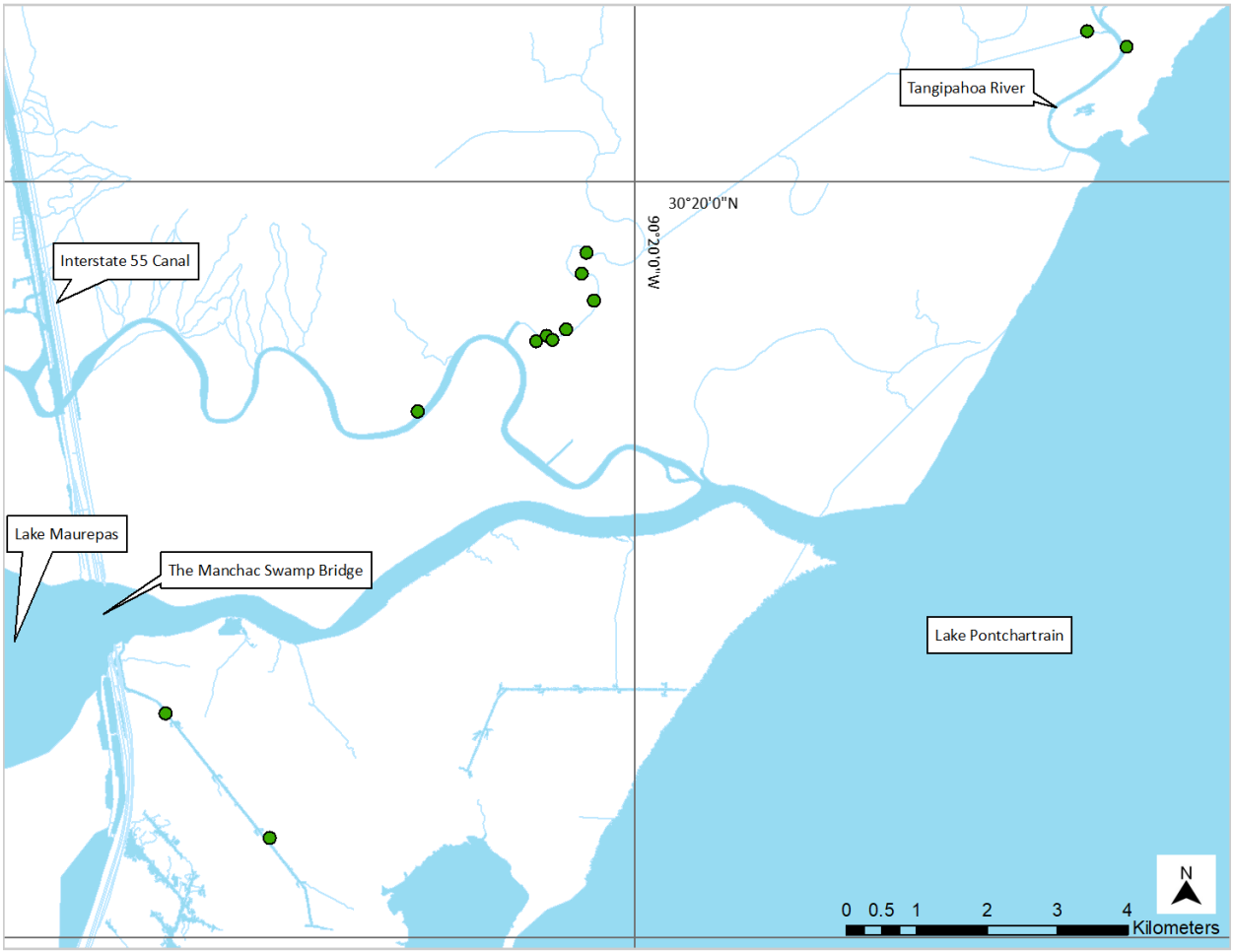

Figure A1. Map of the Lake Pontchartrain Basin Foundation (LPBF) sapling plantings where soil samples were collected.

Compared to the Joyce Wildlife Management Area points LPBF plantings had lower overall average proportion of LOI and phosphorus but higher magnesium and sodium (Figure A2). The sulfur was similar between the two sites (Figure A2). While the LPBF sites were closer

to Lake Pontchartrain and so closer to the influx of sea water they were also closer to the canals for ease of planting and so the seawater might have been better able to wash out leading to not as large of effects.

Figure A2. The concentrations of elements (mg/kg) and proportion LOI overall averages for the 12 LPBF planting sites and all 60 of the Joyce Wildlife Management Area sites.

The sapling data collected was not enough to definitively determine the suitability of sites for growth. The salinity measurements were, on average, higher than those collected for the mature cypress and so the saplings were planted in the zone were there appears to be some adjustment by mature trees to deal with the higher salinity concentrations. It is not yet certain if the saplings will be able to compensate for the high salinities. This research did not reveal a directive for the best planting conditions but more data collected over a longer period of time might disclose something about the ability of cypress saplings to survive in higher saline areas.

APPENDIX B. LDWF GROWTH MONITORING PLOTS

Soil samples and conductivity measurements were taken at four forest growth monitoring plots (GMP) maintained by Louisiana Department of Fish and Wildlife (LDWF). Soil was collected from four GMPs in November 2019 (Table B1). The GMPs had data collected in 2007 and again in 2017. The first plot had 4 cypress with an average growth of 2.2 cm in diameter the second did not have any cypress, the third three trees with an average growth of 4.1 cm diameter and the fourth only one cypress with a growth of 3.0 diameter. While interesting there is not enough data to have significance.

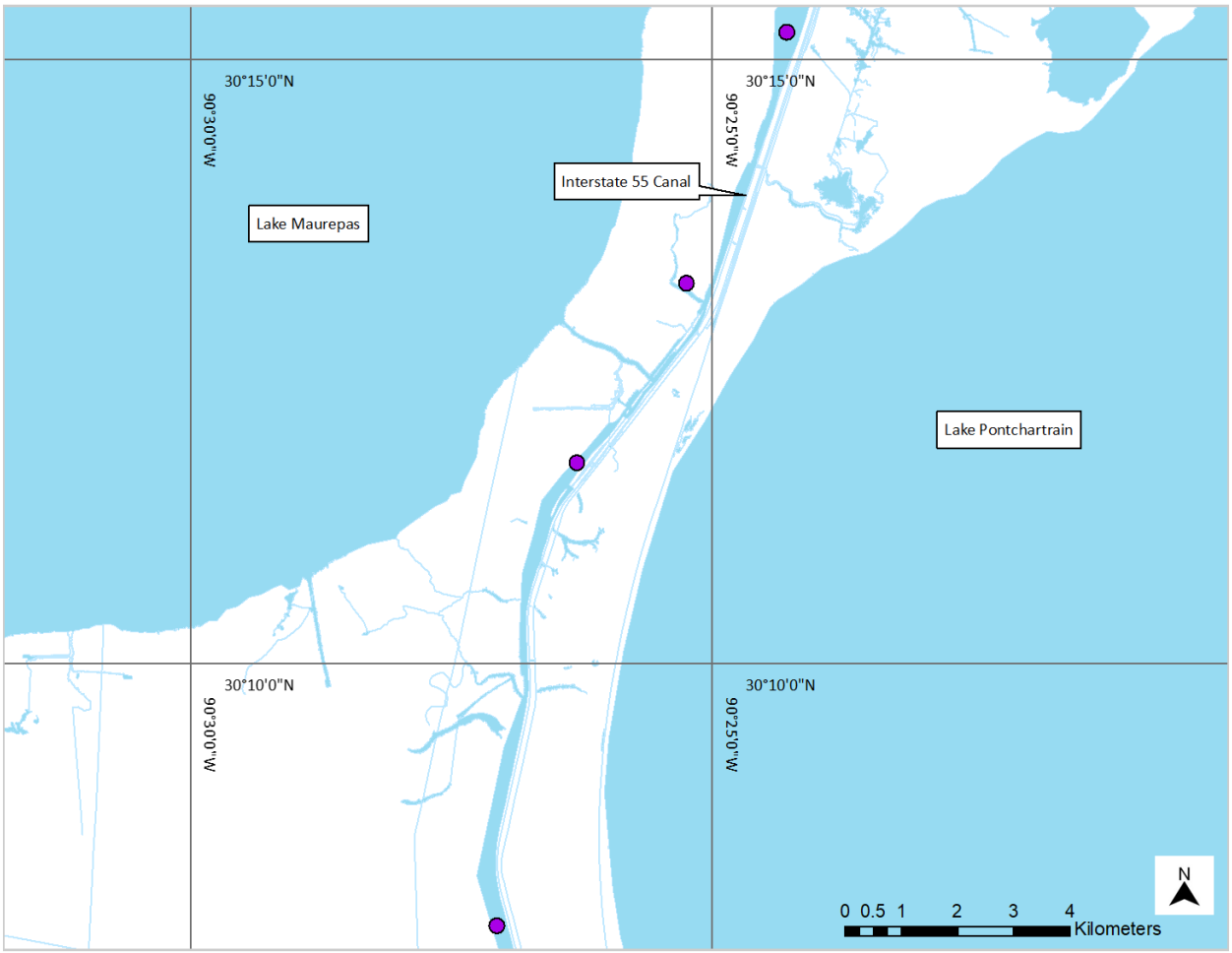

Figure B1. Map of the Louisiana Department of Wildlife and Fisheries Growth Monitoring Plots where soil samples were collected.

Table B1. Louisiana Department of Wildlife and Fisheries Growth Monitoring Plots tree growth data (change in diameter in cm) and soil data as measured with Melich3.

Plot	LOI (proportion)	Ca (mg/kg)	Mg (mg/kg)	P (mg/kg)	K (mg/kg)	Na (mg/kg)	S (mg/kg)
1	0.56	2284.74	2407.99	46.83	356.63	1627.80	364.39
2	0.70	2504.86	1841.66	36.10	231.75	1226.26	720.08
3	0.40	2174.44	1642.50	38.62	494.66	1337.78	118.92
4	0.33	2948.33	1328.76	23.34	350.47	649.41	111.51

The Louisiana Department of Wildlife and Fisheries Growth Monitoring Plots provided an interesting resource but there was not enough data provided from only three plots with cypress growth data to make any large conclusions. Compared to the Joyce Wildlife Management Area average measurements the LDWF plots, on average, had lower LOI proportion and lower phosphorus but higher magnesium and sodium (Figure B2). The sulfur was about the same for both sites (Figure B2). This seems to indicate that the plant nutrients that were stored in the organic content are lower but the area might be more exposed to the seawater intrusion; however, there was not sufficient data to make any conclusions.

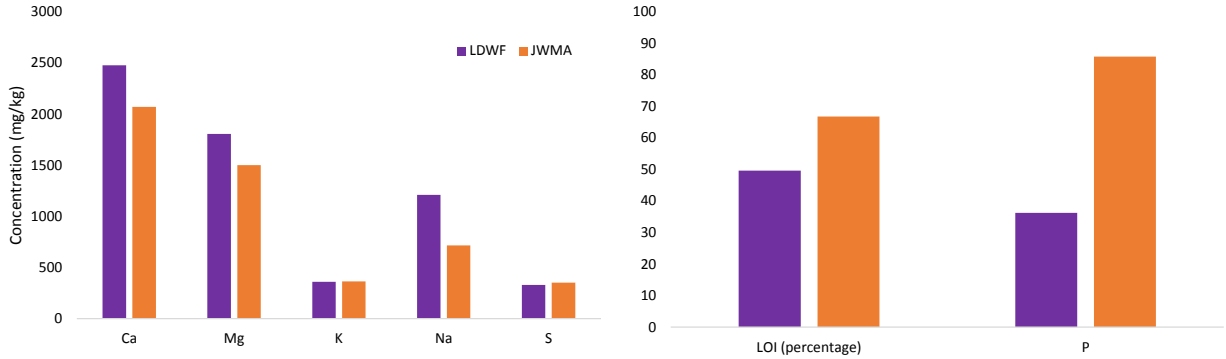

Figure 37. The concentrations of elements (mg/kg) and the proportion LOI overall averages for the 4 LDWF growth monitoring plots and all 60 of the Joyce Wildlife Management Area sites.

APPENDIX C. PHOTOS

Figure C1. Saplings at a Lake Pontchartrain Basin Foundation planting sites in a variety of conditions and sizes.

Figure C2 and AX. There was variability in the vegetation around the cypress sample tree but almost all sites had standing water. Photo credit: Britt Fleming.

Figure C3. Left: often two boats were used to access the sites where a larger motorized boat would go as far as it could followed by a smaller hand paddled vessel. Right: a few of the sites had a root mat on top. Photo credit: Britt Fleming.

Figure C4. Left: A low density site on the edge of the forest to marsh transition. Right: A high density site (the orange vest is where the sample tree is located).

Figure C5. The diameter and cores were taken at normal diameter (18 inches/46 cm above the last buttressing).

APPENDIX D. DATA

Table D1. Site information.

Tree	Lat.	Long.	Date	DBH (cm)	SDI10	SDI20	Esap10	Esap7	ARSTAN ISC	PC Tree Score
10	30.354125	-90.298671	2/18/2019	35.4	0.00	0.00	0.00681	0.00778	0.350	-2.1854
11	30.354610	-90.298221	2/18/2019	29.3	0.00	0.00	0.01571	0.01879	0.689	-1.7002
12	30.354139	-90.303685	2/18/2019	36.1	19.50	38.92	0.02059	0.02110	0.714	-4.3313
13	30.372350	-90.301401	3/1/2019	45.8	133.29	159.22	0.02269	0.02631	0.638	-2.9191
14	30.373293	-90.303279	3/1/2019	40.2	153.92	130.70	0.01985	0.02211	0.648	-5.7495
15	30.384896	-90.322905	3/6/2019	41.3	546.02	649.70	0.03924	0.02401	0.186	3.8943
16	30.385455	-90.324621	3/6/2019	37.1	465.91	129.92	0.04965	0.04461	0.234	8.8710
17	30.386348	-90.326919	3/6/2019	41.3	338.41	375.33	0.03938	0.03370	0.334	10.4567
18	30.380944	-90.314349	3/18/2019	43.6	528.68	702.20	0.02851	0.02442	0.497	0.1642
19	30.379269	-90.313595	3/18/2019	41.5	169.29	67.41	0.04395	0.03731	0.607	2.3640
20	30.379378	-90.313579	3/18/2019	44.7	287.94	258.83	0.02691	0.02523	0.496	-2.8220
21	30.380898	-90.302280	3/13/2019	38.4	138.99	46.95	0.04406	0.05071	0.022	-1.7084
22	30.380564	-90.302977	3/13/2019	47.6	43.95	0.00	0.03197	0.03360	0.503	-1.3917
23	30.380340	-90.304874	3/13/2019	43.7	131.86	117.38	0.01958	0.01913	0.638	-3.1769
24	30.380325	-90.292139	3/18/2019	36.1	0.00	0.00	0.02436	0.02481	0.716	2.9031
25	30.378855	-90.291450	3/18/2019	27.5	19.28	0.00	0.02699	0.02565	0.452	-4.4269
26	30.380346	-90.289886	3/18/2019	39.1	41.37	37.56	0.01835	0.02065	0.444	-1.3603
27	30.381395	-90.290541	3/18/2019	35.8	127.23	0.00	0.03867	0.04155	0.577	-1.0645
28	30.380038	-90.323053	3/20/2019	35.1	142.06	222.17	0.05340	0.06216	0.524	4.3503
29	30.379123	-90.323437	3/20/2019	26.1	144.72	29.70	0.07756	0.08047	0.566	0.5932
30	30.377911	-90.323427	3/20/2019	32.4	191.64	397.41	0.07426	0.08641	0.145	1.6720
31	30.383137	-90.291614	3/22/2019	45.3	367.97	487.66	0.03950	0.04515	0.673	3.5594
32	30.383792	-90.291588	3/22/2019	48	236.39	360.94	0.01881	0.01807	0.571	0.9243
33	30.384811	-90.291190	3/22/2019	33.8	588.96	564.10	0.05024	0.05142	0.672	-1.7278

table cont'd

Tree	Lat.	Long.	Date	DBH (cm)	SDI10	SDI20	Esap10	Esap7	ARSTAN ISC	PC Tree Score
34	30.356094	-90.299399	4/3/2019	27.8	38.49	38.04	0.01506	0.01830	0.381	-0.6324
35	30.357411	-90.299573	4/3/2019	34	82.26	126.07	0.00302	0.00322	0.625	0.9449
36	30.359355	-90.300060	4/3/2019	36.4	23.72	47.33	0.02554	0.02808	0.548	0.2877
37	30.360780	-90.300163	4/3/2019	49.6	116.47	0.00	0.03329	0.03713	0.536	1.7839
38	30.396050	-90.424506	4/8/2019	31.6	300.50	193.90	0.11569	0.13272	0.627	1.8731
39	30.395571	-90.424338	4/8/2019	40.5	100.43	49.16	0.04877	0.05638	0.294	2.8324
40	30.396735	-90.323939	4/10/2019	51.9	428.69	354.65	0.04422	0.03353	0.492	10.7471
41	30.395569	-90.324004	4/10/2019	62	194.13	216.21	0.02791	0.02860	0.138	20.1441
42	30.395997	-90.324575	4/10/2019	38.5	239.47	275.62	0.05443	0.04642	0.313	3.7436
43	30.398337	-90.317191	4/15/2019	39.8	583.75	894.90	0.04651	0.04858	0.186	1.2489
44	30.398985	-90.316600	4/15/2019	62	349.35	426.92	0.02574	0.02770	0.404	4.8188
45	30.397970	-90.315603	4/15/2019	47.5	541.25	427.10	0.03348	0.03219	0.090	3.1105
46	30.397548	-90.316726	4/15/2019	47.4	271.43	192.00	0.03211	0.03279	0.376	11.4659
47	30.404813	-90.448623	4/17/2019	51.8	432.20	622.64	0.02878	0.03205	0.278	4.0051
48	30.404875	-90.449308	4/17/2019	35.9	381.88	198.49	0.04078	0.04584	0.302	1.3745
49	30.384271	-90.285059	4/22/2019	39.9	38.90	38.10	0.01422	0.01655	0.511	-3.7025
50	30.384108	-90.283947	4/22/2019	25	0.00	0.00	0.01217	0.01265	0.636	-5.7782
51	30.384336	-90.282603	4/22/2019	19	0.00	0.00	0.04134	0.05123	0.608	-7.4056
52	30.384404	-90.281724	4/22/2019	18.4	0.00	0.00	0.04412	0.05488	0.584	-7.3529
53	30.350024	-90.335633	4/24/2019	22.4	19.54	0.00	0.08185	0.10380	0.458	-3.7652
54	30.350306	-90.335210	4/24/2019	31.6	197.44	280.98	0.04119	0.05057	0.616	-0.6679
55	30.349720	-90.336535	4/24/2019	12.9	0.00	0.00	0.05927	0.07661	0.281	-7.6327
56	30.352393	-90.338923	4/26/2019	21.1	80.35	107.85	0.14821	0.19317	0.631	-5.0494
57	30.353268	-90.339387	4/26/2019	27.8	45.45	90.69	0.04272	0.04866	0.510	-1.3244
58	30.354059	-90.339081	4/26/2019	21.8	50.49	99.99	0.04258	0.04897	0.656	-5.3672
59	30.351835	-90.340001	4/26/2019	24.9	0.00	0.00	0.05842	0.06510	0.399	-2.8222
60	30.405662	-90.402603	5/1/2019	51.8	508.56	523.73	0.02777	0.02937	0.393	2.4661

table cont’d

Tree	Lat.	Long.	Date	DBH (cm)	SDI10	SDI20	Esap10	Esap7	ARSTAN ISC	PC Tree Score
61	30.405258	-90.402023	5/1/2019	36.2	1042.90	1257.03	0.01862	0.01776	0.564	-4.6664
62	30.355238	-90.339087	5/3/2019	26.1	296.82	312.35	0.05219	0.06185	0.513	-1.5085
63	30.356076	-90.339025	5/3/2019	35	286.31	214.29	0.06661	0.07695	0.569	4.9100
64	30.356330	-90.338543	5/3/2019	31.6	253.83	116.23	0.08951	0.10208	0.686	1.8236
65	30.385370	-90.286510	5/6/2019	34.9	413.09	214.74	0.04653	0.04940	0.440	-1.8351
66	30.385899	-90.287338	5/6/2019	30	348.89	397.52	0.04614	0.05349	0.43	-5.5177
67	30.386386	-90.287865	5/6/2019	25.7	548.26	518.30			0.57	
68	30.377709	-90.283509	5/21/2019	23.6	0.00	0.00	0.01627	0.01578	0.08	-6.5660
69	30.377030	-90.284105	5/21/2019	27.4	0.00	0.00	0.01079	0.01291	0.53	-5.9646
70	30.376190	-90.284567	5/21/2019	32.6	0.00	0.00	0.01099	0.01278	0.51	-5.2095

Table D2. Basal area increment information. The cores for tree 67 were not readable.

Tree	BAI10 (mm)	BAI7 (mm)	Slope5	Slope7	Slope10	Slope15	Slope20	Slope25	Slope30	Slope35	Slope40
10	1930.22	1542.35	9	17	16	10	-33	-105	-79	-55	-71
11	4822.90	4036.08	45	68	63	21	-11	-99	-93	-64	-71
12	6025.55	4321.10	53	52	24	-5	1	-33	-50	-24	-21
13	7677.17	6231.53	95	-71	30	17	18	-4	-9	-7	-6
14	5886.16	4590.23	68	89	61	33	33	6	-8	-3	-9
15	24880.22	10655.32	-289	-274	-532	-154	-11	-14	-19	8	17
16	29937.64	18829.27	179	84	-126	-129	-79	-60	-41	0	35
17	28565.83	17108.24	20	66	-185	-122	-138	-50	-20	24	28
18	16544.06	9918.13	149	98	-46	22	-9	-23	-39	-4	6
19	21559.57	12812.81	298	58	-138	-132	-49	-12	12	40	34
20	12531.44	8224.62	-98	-61	-49	25	29	35	20	17	5
21	17245.37	13892.82	258	308	213	99	88	38	18	20	18
22	15253.00	11220.11	2	-37	30	15	35	23	15	25	27

table cont’d

Tree	BAI10 (mm)	BAI7 (mm)	Slope5	Slope7	Slope10	Slope15	Slope20	Slope25	Slope30	Slope35	Slope40
23	11254.23	7694.89	-56	10	-9	-21	-2	12	12	21	15
24	12610.96	8991.42	238	128	53	3	-21	-43	-45	-56	-54
25	5565.11	3702.00	129	53	8	-2	-35	-49	-56	-42	-33
26	9156.47	7212.00	215	160	102	27	21	-8	-20	-29	-29
27	15642.18	11767.23	74	140	103	67	30	10	3	11	8
28	30670.23	24990.39	313	236	295	119	137	111	59	55	32
29	24546.87	17827.41	-77	95	68	-19	-24	-19	-37	-20	0
30	28100.58	22887.92	18	349	314	129	86	12	-44	-25	-18
31	20966.39	16773.04	649	366	244	135	58	8	7	16	7
32	11685.67	7855.68	27	-13	-29	-20	6	-5	-23	-10	-9
33	18536.83	13282.47	101	71	43	48	44	37	21	22	20
34	4828.40	4107.82	10	45	57	11	15	-92	-124	-89	-87
35	1180.47	882.29	16	10	7	-23	-25	-115	-135	-108	-107
36	9534.62	7337.57	70	116	82	-1	-13	-50	-75	-49	-50
37	16089.07	12559.14	69	133	118	54	42	-1	4	20	13
38	42876.16	34430.61	-304	-127	232	297	231	173	120	100	74
39	22117.34	17899.75	-30	-62	129	134	89	60	13	9	-7
40	26781.14	14215.49	216	-62	-321	-76	-30	4	2	17	9
41	28671.91	20566.88	85	369	170	-13	-68	-15	-12	10	21
42	27743.48	16564.33	-3	137	-154	-78	-46	-6	38	46	38
43	16757.19	12253.82	60	-33	21	-6	-23	-9	-21	-6	-9
44	19439.35	14645.59	151	63	84	87	18	9	13	26	14
45	20465.28	13774.06	181	304	72	64	35	19	5	13	8
46	26432.39	18892.17	295	181	80	80	57	40	-18	-1	7
47	17655.03	13763.38	-261	23	101	108	46	3	-9	4	5
48	13111.29	10316.46	-30	49	85	35	13	-32	-79	-60	-51
49	4877.94	3975.37	42	31	44	2	0	-34	-32	-21	-22
50	2827.78	2058.01	37	30	11	-30	-16	-36	-36	-29	-35

table cont’d

Tree	BAI10 (mm)	BAI7 (mm)	Slope5	Slope7	Slope10	Slope15	Slope20	Slope25	Slope30	Slope35	Slope40
51	4154.72	3603.45	15	56	62	27	19	-26	-34	-18	-11
52	3996.07	3479.53	19	54	60	21	12	-37	-56	-28	-20
53	18375.40	16311.81	-476	167	268	199	131	-82	-48	-2	-18
54	13377.38	11494.70	160	135	180	97	56	-35	-80	-41	-45
55	3775.20	3415.94	-134	36	59	45	8	-53	-71	-36	-36
56	22621.83	20638.50	-546	-148	243	131	107	31	-8	22	24
57	12799.41	10204.31	-56	-39	57	-34	20	-56	-86	-42	-54
58	5895.76	4745.82	10	18	41	8	-3	-81	-85	-71	-61
59	16215.90	12648.71	-289	-33	63	44	32	-70	-45	-17	-15
60	14272.34	10568.50	-102	-118	-9	-26	-3	4	-6	-3	-4
61	5290.43	3532.06	-100	-3	-11	-10	-12	-14	-15	-14	-23
62	11194.98	9287.09	100	185	143	-9	9	-103	-133	-98	-59
63	29170.14	23588.04	1045	864	471	149	141	9	-54	-8	8
64	32264.68	25756.45	-20	132	221	165	151	58	28	29	30
65	13790.07	10248.91	314	167	88	19	0	-10	-15	-7	-3
66	11059.82	8976.04	-133	-83	48	57	43	26	20	22	15
67											
68	2471.57	1678.65	-17	0	-9	-22	-26	-65	-50	-28	-19
69	2672.60	2238.49	-35	25	29	-24	-33	-68	-69	-46	-36
70	3364.78	2740.50	162	110	60	6	-17	-54	-52	-45	-29

Table D3. Soil concentration measurements at the surface with Melich 3.

Site	Ca (mg/kg)	Cu (mg/kg)	Mg (mg/kg)	P (mg/kg)	K (mg/kg)	Na (mg/kg)	S (mg/kg)	Zn (mg/kg)
10	2975.0818	7.47848	1816.7646	89.5479	342.7767	1364.8821	306.6673	17.5700
11	2626.6974	1.20792	1757.8996	101.9393	423.2174	803.9513	176.6642	10.2562
12	2646.3854	1.67600	1895.6914	198.8830	889.2126	1814.5254	521.3880	12.9162
13	2312.3723	1.37116	1273.9037	94.7230	443.6235	448.0374	154.4972	10.5886
14	1907.1455	1.48957	1246.0919	48.4632	366.1351	598.3168	170.6397	6.4606

table cont’d

Site	Ca (mg/kg)	Cu (mg/kg)	Mg (mg/kg)	P (mg/kg)	K (mg/kg)	Na (mg/kg)	S (mg/kg)	Zn (mg/kg)
15	2551.8761	1.90374	637.5965	52.7166	303.6383	218.5454	82.8348	17.4852
16	2900.0359	1.82208	978.9077	81.4408	549.4634	165.7894	56.3572	15.6642
17	2771.7469	2.03109	748.1277	83.3899	567.5283	196.3416	195.6812	16.6220
18	2968.0965	1.60642	972.8361	65.9904	465.4701	290.4052	92.1301	13.3733
19	3607.1885	1.90213	1148.4533	90.5221	672.2664	303.3656	124.1299	12.7491
20	2540.1970	1.43402	1018.2182	82.2281	620.2398	456.3363	94.4299	9.4239
21	2665.8807	1.91605	1169.3902	91.2067	507.7358	369.4586	103.4063	11.1777
22	2789.0985	1.25630	1248.2539	45.8822	325.7885	435.2826	152.4033	9.6098
23	2537.8206	1.04660	991.3412	55.1732	285.5550	492.2524	393.3714	11.1222
24	2308.8223	1.87615	1118.0885	94.6854	749.8135	817.5885	134.3031	7.8362
25	2519.9085	2.70269	868.2442	122.2681	339.4508	672.8989	94.2665	14.7889
26	1815.1003	1.93838	1042.2238	71.6968	424.1654	548.7703	99.9708	12.1730
27	2950.3888	5.98000	1188.3453	113.7632	691.6375	760.5533	122.4635	17.8119
28	2563.7086	2.21494	1666.5522	77.5967	355.6413	363.7873	135.7747	10.7760
29	2323.0005	1.45610	1502.0429	33.8876	301.1412	723.5351	967.8105	12.3720
30	3188.5920	1.64400	1137.4428	98.8577	518.7544	243.9252	98.3162	9.9184
31	3225.5862	1.65308	1178.6021	73.6059	344.1580	592.2441	110.2815	13.6459
32	2508.4654	1.57944	1308.5699	92.9211	436.7217	664.6544	122.4392	10.0789
33	3032.0137	1.55421	1506.0866	87.1616	342.4818	598.9055	95.2413	11.4055
34	2674.4878	1.46340	1611.5986	186.5216	840.8554	1448.8768	405.4548	12.8934
35	3092.7361	1.66140	2096.7147	201.9384	484.6902	1192.8130	257.5677	10.5679
36	3224.5667	6.02000	1747.1595	397.6097	1341.4144	1212.3851	171.3277	8.9174
37	3088.6621	1.46571	1548.6454	110.1507	409.6514	711.4804	140.9910	8.4375
38	3420.0666	5.87836	1575.4630	142.9082	298.1620	1448.9521	256.0377	11.1131
39	3933.4017	3.57667	1722.2121	549.7558	692.0225	1448.6188	141.0813	8.6038
40	1988.8928	2.77451	651.8373	93.3641	681.7312	150.7377	65.5996	16.3341
41	2564.7096	2.78000	682.7790	86.0407	722.5864	167.9566	84.3513	24.2669

table cont’d

Site	Ca (mg/kg)	Cu (mg/kg)	Mg (mg/kg)	P (mg/kg)	K (mg/kg)	Na (mg/kg)	S (mg/kg)	Zn (mg/kg)
42	2055.6705	2.86061	461.4400	135.5075	793.5562	263.0053	116.0449	24.2281
43	1935.0662	2.68623	403.6133	97.3266	505.5182	136.0842	39.0837	22.6604
44	2180.4381	3.75562	452.1354	89.6698	544.9617	160.2035	39.5650	27.1433
45	2501.4067	2.30079	612.3687	108.3849	455.7583	140.3659	42.6054	28.5141
46	1373.9458	2.25110	320.4484	61.1321	229.1393	73.8507	27.8622	11.0349
47	4529.9486	3.00944	1745.6167	199.7164	568.4594	649.9611	66.2758	14.4011
48	3725.8308	1.89568	1242.3714	101.6441	376.9873	619.9811	86.9624	11.5492
49	1984.4148	2.74141	1398.6327	50.4461	236.2327	1042.4438	206.9960	10.4845
50	2280.0309	1.21481	1795.3933	116.1860	1166.4431	1332.7753	311.3725	11.3569
51	2344.4398	3.16333	1718.0333	154.6510	1727.7747	1190.7333	591.9673	12.9743
52	2703.6448	15.14522	1678.6883	211.6217	1154.7944	1661.9639	410.3487	18.6774
53	3247.9125	16.92219	2061.0900	239.7034	790.1494	1160.5344	410.5547	9.7700
54	2302.0321	1.60536	1824.4143	127.6111	458.8389	635.7382	225.6804	4.3100
55	3225.8811	3.74987	2387.2328	201.9096	583.2509	848.0837	532.0979	4.9565
56	2984.2585	0.85537	2256.6285	184.6924	494.8290	536.3268	224.2605	4.9693
57	3281.0543	2.74192	2095.3627	261.0093	971.2392	626.3258	264.9890	6.1764
58	3268.7702	4.67661	1861.9354	115.3286	433.9007	468.2409	318.3866	10.4748
59	2912.2148	9.22182	1908.6548	314.9081	1236.8221	992.7813	295.7797	9.8803
60	2226.6196	3.39596	1320.1536	54.5898	153.5392	409.4396	163.4798	20.3179
61	1975.6287	1.46000	884.4433	34.0058	179.0843	355.5530	119.0297	16.8948
62	2992.6597	7.82132	2086.2879	129.2661	515.0468	535.0474	251.0161	13.3200
63	2006.7875	2.06969	1240.5122	82.5244	447.7600	403.9841	141.5406	3.8719
64	2953.2664	10.09956	1980.5688	93.2218	486.9070	398.4110	470.2288	11.0855
65	2173.0545	2.47505	1340.2543	57.3273	234.5484	624.1989	206.4519	8.5629
66	2345.7710	15.54082	1743.9988	57.1998	290.3735	973.0825	414.8349	15.6390
67	2723.7439	9.21944	1416.1217	47.9922	185.9600	567.7569	401.7592	16.4236
68	2441.5527	16.23500	1344.6664	121.7550	400.8309	814.5886	459.4555	22.3505

table cont’d

Site	Ca (mg/kg)	Cu (mg/kg)	Mg (mg/kg)	P (mg/kg)	K (mg/kg)	Na (mg/kg)	S (mg/kg)	Zn (mg/kg)
69	2408.6303	2.62714	1546.6351	210.2531	852.1246	505.6543	299.3006	11.8594
70	2114.6008	1.73892	1358.6322	83.0638	614.8076	612.1138	416.7970	14.6030

Table D5. Conductivity, loss on ignition (LOI), and soil concentration measurements at the surface with DTPA. Sites 15, 16, and 17 do not have conductivity measurements.

Site	Conductivity ($\mu S\ cm^{-1}$)	LOI (proportion)	Cu (mg/kg)	Fe (mg/kg)	Mn (mg/kg)	Zn (mg/kg)
10	647.0	0.8074	4.2267	401.0239	126.2628	28.1956
11	264.2	0.8057	1.9367	362.6830	68.2170	28.8969
12	370.7	0.8119	2.4250	246.3481	81.0641	18.4545
13	67.2	0.6923	1.6745	610.6745	171.3226	11.9981
14	72.4	0.7645	1.4230	543.4235	180.0850	10.3028
15		0.5840	3.0209	498.2899	976.1055	24.0222
16		0.6043	2.7760	505.3029	796.9188	20.7410
17		0.5814	2.8853	437.6462	838.3448	23.5443
18	55.0	0.7379	2.2159	501.9898	495.4778	18.3842
19	55.2	0.7279	2.2907	575.6407	528.1659	16.4671
20	61.6	0.7869	2.4216	685.2238	419.4078	14.8727
21	50.9	0.7333	2.2360	656.4248	416.8096	18.4240
22	68.6	0.7162	1.8730	610.5552	293.2813	15.5795
23	111.3	0.7377	2.2000	603.4711	424.2569	20.3500
24	95.3	0.8071	2.0242	564.4567	480.9093	18.1712
25	245.7	0.6973	3.4822	546.8960	318.3183	20.8723
26	62.0	0.6382	2.4661	519.9870	273.0449	18.1681
27	70.3	0.7955	4.0283	473.6798	568.3266	21.0827
28	65.4	0.7247	2.4007	572.2234	591.2822	17.4510
29	97.2	0.7585	2.1403	697.1579	364.0991	18.4920

table cont'd

Site	Conductivity ($\mu S\ cm^{-1}$)	LOI (proportion)	Cu (mg/kg)	Fe (mg/kg)	Mn (mg/kg)	Zn (mg/kg)
30	63.5	0.7797	2.3706	557.3174	391.4872	17.9317
31	147.0	0.7795	2.0945	563.6495	249.4934	17.9745
32	158.4	0.8199	4.8743	385.9185	190.2562	16.2163
33	141.4	0.8228	1.7741	401.4481	190.6179	15.3745
34	214.4	0.8212	2.2338	382.0566	70.0219	19.2456
35	293.8	0.8298	2.2724	290.8020	77.6961	23.7701
36	126.1	0.8388	4.8908	273.8705	85.3179	13.1335
37	188.1	0.8278	2.0180	322.5525	92.9014	12.4784
38	257.9	0.8723	4.3061	94.9465	117.8318	15.6030
39	254.5	0.8976	2.3541	110.3044	71.9385	12.2733
40	52.4	0.4595	3.1756	561.5500	906.4592	21.5744
41	71.7	0.4426	3.3221	518.3182	704.1594	25.5336
42	81.4	0.5055	3.3631	558.8094	954.8968	32.2015
43	86.8	0.3347	3.6522	466.4601	600.6776	27.6500
44	74.9	0.3794	3.3855	510.3674	1295.1690	29.7936
45	66.3	0.3675	2.9506	430.6470	1019.9257	29.3794
46	75.3	0.3289	2.5714	385.1869	711.5168	20.7472
47	146.4	0.7741	2.3281	560.7226	193.0055	11.8194
48	148.9	0.8711	1.8498	447.4374	175.7934	14.1801
49	216.9	0.7246	2.3746	581.9090	84.8891	15.8901
50	301.4	0.7886	1.4681	333.8805	59.9580	18.4840
51	216.9	0.8211	3.4257	476.7806	65.1005	19.6681
52	455.0	0.8049	3.4636	346.6977	44.9699	15.2630
53	86.4	0.8172	15.1000	446.6529	74.5903	11.6976
54	86.3	0.8551	1.5392	392.5576	56.9157	6.2415
55	118.2	0.8163	3.0730	394.1061	33.3892	6.3980
56	46.2	0.8402	2.0552	511.3984	73.1081	7.5077

table cont’d

Site	Conductivity ($\mu S\ cm^{-1}$)	LOI (proportion)	Cu (mg/kg)	Fe (mg/kg)	Mn (mg/kg)	Zn (mg/kg)
57	55.6	0.7994	4.4783	637.2400	119.2463	9.1446
58	84.7	0.7918	8.8664	640.7367	270.4997	15.9642
59	54.4	0.7696	9.6887	467.4720	55.2268	12.6464
60	103.3	0.5959	4.5150	491.9997	269.5813	32.0073
61	117.1	0.6951	20.4930	560.1184	459.2541	36.1077
62	76.0	0.7970	7.7213	466.5250	132.9759	18.8542
63	56.4	0.8294	3.4567	502.1058	152.3031	11.5505
64	80.5	0.8039	18.1058	603.2710	177.8101	19.7630
65	200.2	0.6982	3.9379	453.5471	202.2844	15.5228
66	266.2	0.7962	13.2251	508.9357	277.3618	25.2834
67	161.5	0.7934	14.7807	446.1441	339.0740	38.8689
68	106.0	0.6310	4.8861	637.7236	96.3661	20.1929
69	62.5	0.7823	3.9407	412.0797	112.0898	15.1492
70	71.0	0.7709	2.9316	386.3230	79.6775	22.7952

Table D6. Soil concentration measurements at the 30 cm depth with Melich 3.

Site	Ca (mg/kg)	Cu (mg/kg)	Mg (mg/kg)	P (mg/kg)	K (mg/kg)	Na (mg/kg)	S (mg/kg)	Zn (mg/kg)
10	2.3003	2793.0639	4.2600	32.3766	199.0406	1522.4158	1978.2468	22.8355
11	1.4270	2142.5295	4.6800	31.1815	197.1495	854.2155	828.6128	9.8510
12	0.3318	2463.9874	3.4100	28.1518	357.6348	1995.1252	2315.2279	26.8454
13	1.0514	1465.2041	4.4500	36.8608	179.5694	536.3353	713.9693	5.5610
14	1.6911	1922.3178	4.4000	44.8284	171.8340	921.5327	853.0620	5.4942
15	2.2600	977.8926	4.8700	47.6566	333.1338	185.6081	120.5453	9.8122
16	1.0274	827.0869	4.3300	22.9387	87.4515	280.3803	170.0897	8.8766
17	1.6792	840.5765	4.5400	24.6370	206.2192	285.4419	128.9632	7.6003
18	1.0661	1229.7833	4.4900	19. 5486	113.4868	373.9464	565.9075	11.7558

table cont’d

Site	Ca (mg/kg)	Cu (mg/kg)	Mg (mg/kg)	P (mg/kg)	K (mg/kg)	Na (mg/kg)	S (mg/kg)	Zn (mg/kg)
19	1.2230	1298.1808	4.3000	31.5390	148.1902	599.6552	470.4184	5.5166
20	1.2296	1454.9826	5.0300	32.4808	168.1786	759.5483	169.2103	3.2432
21	1.3252	1974.0236	4.1600	29.7469	148.0776	636.6576	1377.7016	8.1755
22	2.0779	1911.4249	4.6100	38.1012	122.9164	465.2946	585.6418	28.3827
23	0.9206	1849.9477	4.4300	21.4264	148.0547	973.3765	761.4923	9.9505
24	2.2495	1782.5023	4.6900	41.8853	182.5210	996.6702	216.5430	7.7521
25	1.8415	1743.5400	4.6000	49.4813	147.5132	1037.0234	333.1792	9.3260
26	1.9212	1998.0887	4.5100	35.0318	179.8537	1211.4353	471.6172	11.2445
27	1.4196	1900.6005	4.7300	24.3666	201.2564	1895.0963	681.6713	9.3720
28	1.7573	1481.1621	4.5500	38.0580	197.2990	370.2949	636.6462	10.1337
29	1.5951	2137.2199	4.9000	32.1266	268.0213	823.1531	457.0296	10.8883
30	1.9107	1836.9917	4.9800	51.9164	285.4086	862.8440	354.4889	6.7138
31	1.2718	2033.5571	4.3300	32.5129	202.0713	1123.4994	719.6456	9.6554
32	1.4489	2132.9164	4.6500	32.1224	220.5646	1801.2164	589.7584	9.2402
33	1.5422	1973.8527	4.5900	33.7386	165.8005	823.7562	407.7727	9.9465
34	1.3191	2347.4739	4.9000	48.3984	239.7000	1802.4377	499.5934	7.4602
35	1.3693	2118.5781	4.7400	37.9963	144.1756	736.8100	596.1100	12.8173
36	2.6796	1771.6379	4.8500	66.1563	221.6033	978.5954	293.1917	8.2029
37	1.3885	1752.5728	4.9400	36.8585	126.1121	1048.2387	164.1638	4.8196
38	2.5546	2841.0484	5.6100	85.8860	321.1158	1423.0996	298.3806	15.9872
39	2.3228	1910.1805	4.8900	64.3519	274.2732	1194.3420	812.0653	21.8529
40	1.6537	610.1592	4.6300	40.9220	295.3883	144.4726	85.8250	9.5293
41	2.9718	682.7333	4.7700	61.9986	430.5538	170.2629	142.6749	17.7367
42	0.5990	642.7738	4.2500	33.0332	213.4573	352.2479	113.2128	17.0736
43	1.4420	430.1386	4.6800	28.9792	122.9543	101.5558	19.6302	12.7451
44	1.8773	536.4549	4.5900	40.3720	181.5947	151.3483	41.6975	11.0054
45	1.3698	658.7725	4.6100	27.1263	182.8411	131.1550	34.4559	15.3433

table cont’d

Site	Ca (mg/kg)	Cu (mg/kg)	Mg (mg/kg)	P (mg/kg)	K (mg/kg)	Na (mg/kg)	S (mg/kg)	Zn (mg/kg)
46	1.7144	300.8076	4.8500	36.7606	156.2558	72.9913	28.1245	9.1538
47	3.1015	1451.5554	4.9100	49.9207	201.3740	651.8455	216.2588	6.8496
48	1.4824	926.2660	4.6600	26.3510	88.0688	332.1660	325.0379	15.9748
49	1.2510	1839.8440	4.4800	31.6155	157.5848	543.2211	637.3045	8.3589
50	1.2275	2281.8294	4.5400	35.0480	129.0935	1549.9249	638.5231	9.7708
51	1.0969	2032.8046	5.3300	64.2230	135.9817	818.8650	321.0481	5.4370
52	1.4369	2647.8396	5.0900	62.4410	454.5289	3273.9219	584.0988	5.2831
53	1.1089	2439.5136	5.0800	32.5032	270.2252	2208.7732	660.6856	3.6043
54	1.5380	2454.9223	5.0400	65.1261	219.9663	981.4906	429.8643	2.9557
55	0.1824	1228.8457	4.9800	34.2986	141.3067	985.4804	355.6358	0.7279
56	3.3792	2521.1874	5.0200	100.3640	245.7904	1247.9312	458.3213	3.9053
57	1.2024	2672.7942	5.0600	67.2402	255.7933	882.6858	357.3305	2.1581
58	1.8278	3126.0930	4.6600	30.9388	121.6144	790.9372	1258.1054	12.2243
59	1.1103	2243.3290	5.1500	44.9586	170.7636	1090.1419	653.9510	2.6387
60	2.1066	1822.2720	4.9400	32.7309	231.3785	688.2839	309.7086	14.3685
61	1.9574	1940.9046	5.0200	30.7674	263.9722	841.1838	509.7104	12.8468
62	5.3525	2703.2996	4.8800	46.6957	240.7659	528.6127	768.1377	13.7105
63	2.1315	2415.0318	4.6900	28.6474	164.9506	480.6909	1062.0533	4.9450
64	1.6556	2170.5446	5.0700	43.5389	147.9290	346.2708	250.9260	4.8810
65	4.6674	1937.5450	4.8000	31.2962	146.3548	1109.9194	337.1806	7.9830
66	2.6908	2423.6465	4.9900	33.5220	231.4282	1678.0985	578.5672	10.7828
67	1.7399	1867.9050	4.7700	24.3224	118.2792	729.9311	455.9867	7.0761
68	1.2394	1391.6877	4.6500	45.2054	110.0410	583.9497	687.3893	6.2020
69	1.1953	1712.6336	4.4100	46.0436	172.0542	882.1064	1096.5773	8.8561
70	1.1852	1738.0041	4.5000	36.0543	107.8953	733.6362	988.2345	9.3729

Table D7. Conductivity, loss on ignition (LOI), and soil concentration measurements at 30 cm depth with DTPA.

Site	Conductivity ($\mu S\ cm^{-1}$)	LOI (proportion)	Cu (mg/kg)	Fe (mg/kg)	Mn (mg/kg)	Zn (mg/kg)
10	0.7568	3086.5879	2.3809	619.3338	54.5097	24.2416
11	0.7907	2095.5820	1.9624	612.2518	43.5047	18.2259
12	0.7417	2990.7852	1.4909	714.6082	59.2178	34.9365
13	0.6260	1368.7924	1.3861	419.1398	103.6505	7.4792
14	0.6978	1453.2780	1.8454	540.8322	91.9132	11.8075
15	0.5109	1735.0103	2.6369	473.2554	432.3464	13.5902
16	0.4510	936.6275	2.0196	480.7189	234.3424	10.5736
17	0.3983	1076.0655	2.2434	386.1510	171.7636	9.1993
18	0.5704	1360.8738	1.3738	430.2565	69.3874	13.1392
19	0.5723	1029.5076	1.3897	405.7406	66.9814	7.0863
20	0.6118	806.2208	1.8355	371.0049	97.8290	5.2137
21	0.6290	1757.2250	1.6620	555.3195	87.9488	10.9370
22	0.6235	1515.1536	1.5373	411.4329	74.0791	9.4181
23	0.6306	1347.9536	1.3406	510.2338	117.6087	12.4504
24	0.5936	1283.0646	2.2963	497.5967	75.7915	13.0231
25	0.6288	1510.4434	2.5391	512.0866	68.4854	13.1885
26	0.6144	1326.6819	2.7077	679.1583	87.0940	15.8072
27	0.6271	1389.5363	1.9440	477.2579	80.5129	14.1528
28	0.5528	1480.9209	2.3604	447.3502	143.5568	12.2722
29	0.5688	1344.7831	2.6507	338.7806	133.9204	17.2316
30	0.5330	1388.1535	2.7703	340.0494	131.5919	14.7359
31	0.6332	1372.6187	1.8652	463.1515	78.2160	14.9000
32	0.7108	1340.6582	2.2402	420.7356	90.6075	12.8186
33	0.6668	1702.4798	1.9198	309.0500	75.7708	7.5557
34	0.7764	2008.6595	1.6508	165.9066	13.5635	9.3459

table cont’d

Site	Conductivity ($\mu S\ cm^{-1}$)	LOI (proportion)	Cu (mg/kg)	Fe (mg/kg)	Mn (mg/kg)	Zn (mg/kg)
35	0.7980	2617.0466	1.5156	342.5076	46.9387	16.4726
36	0.7720	1896.5242	2.5250	184.8018	14.0201	14.1920
37	0.7563	1565.5151	2.0531	420.7305	48.6500	14.7630
38	0.7985	3043.4534	2.2057	244.8255	137.3856	16.3426
39	0.7923	3158.8286	2.2751	308.6018	111.4453	23.0244
40	0.2865	705.3335	2.0531	416.8695	346.8662	11.1956
41	0.3610	1690.4838	3.1068	418.3463	569.0319	17.5484
42	0.2842	663.0119	1.6785	408.9562	131.2228	16.9531
43	0.1979	501.2620	2.0378	303.4938	271.5031	11.5463
44	0.2022	704.8528	1.9440	306.5678	397.6711	10.5829
45	0.2300	556.5674	1.8818	274.9075	417.2782	12.5110
46	0.1965	842.3361	2.2163	260.1719	443.0026	12.3585
47	0.8082	2325.6682	2.5396	562.3883	101.2544	8.5952
48	0.7641	2060.6731	2.9933	432.0215	91.8560	29.3306
49	0.5655	1648.7742	1.7240	305.4457	41.5042	13.4736
50	0.6352	1791.6606	1.9499	381.3610	35.4826	15.5165
51	0.6097	1732.2188	1.6379	155.6290	20.9276	8.6700
52	0.6387	1918.4684	1.8355	185.0907	18.8383	7.9087
53	0.7163	1709.3611	1.5732	264.3382	38.4189	7.0273
54	0.7773	1969.2605	1.1498	102.3870	45.9096	3.3180
55	0.6625	887.7956	0.8702	72.0335	24.5833	3.3460
56	0.7877	2126.5471	3.8228	144.6357	34.3015	4.3606
57	0.6781	2250.7961	1.4000	214.9478	70.9908	5.1177
58	0.7438	2772.4481	1.9292	310.3297	117.9974	10.7444
59	0.7049	1758.9986	1.3097	187.0929	33.0605	3.9082
60	0.4552	1736.1051	4.0008	419.8115	116.8595	21.4959

table cont’d

Site	Conductivity ($\mu S\ cm^{-1}$)	LOI (proportion)	Cu (mg/kg)	Fe (mg/kg)	Mn (mg/kg)	Zn (mg/kg)
61	0.4873	1642.7804	4.1166	392.9391	152.7225	19.4663
62	0.7412	2257.3305	3.7606	259.2266	115.0452	18.0000
63	0.7887	2181.5258	2.1218	308.6794	126.0427	8.1773
64	0.7657	2222.8362	10.9303	311.3106	111.4034	15.1962
65	0.5833	1204.2322	8.9701	430.2350	84.1548	14.9394
66	0.6442	1552.6825	3.5145	363.1303	126.4771	16.5493
67	0.6717	1332.9236	2.1792	427.1397	133.6090	12.5350
68	0.5519	1268.6174	1.9595	290.7752	36.1302	12.6531
69	0.5575	1476.6964	1.9592	299.2461	36.8598	10.9514
70	0.6362	1630.5085	2.1809	357.1514	37.8436	14.9994

Table D8. Subset of soil samples at the surface with HCl.

Site	P (mg/kg)	As (mg/kg)	Ba (mg/kg)	Be (mg/kg)	Cd (mg/kg)	Co (mg/kg)	Cr (mg/kg)	Cu (mg/kg)	Mn (mg/kg)	Na (mg/kg)	Ni (mg/kg)	Pb (mg/kg)	Si (mg/kg)	Zn (mg/kg)
23	945.0464	4.3853	297.0000	1.4979	4.0333	15.4086	51.5014	15.2272	1172.8391	1208.9542	25.6992	17.6252	322.5232	103.4022
17	975.3106	5.3522	378.4885	1.7610	5.1339	18.7957	62.5035	23.4865	2578.2604	523.1879	34.3387	34.8676	334.7508	126.3127
34	677.5362	5.0272	255.1812	1.0938	4.1021	9.1848	32.1291	12.4819	217.8788	3502.7375	16.8491	12.2901	299.3859	77.8596
61	625.3185	5.9744	306.2885	1.5364	5.9414	18.6718	84.2401	27.6162	1108.6010	1067.4632	29.1323	43.0661	366.7125	129.9313
29	979.941	5.0936	319.2645	1.4037	5.0404	15.1071	44.5595	17.2280	1049.1162	2012.0752	31.5784	26.7682	429.7462	86.1503
19	1242.267	4.5302	370.8776	1.4799	4.0874	14.2139	41.2879	20.3599	1597.8183	937.0326	28.7602	24.3370	446.7469	92.9141
63	892.2961	4.7639	358.5249	1.4137	4.2410	10.7317	73.8136	14.2752	468.3617	1190.8234	25.2997	14.0033	352.3297	58.2318
48	779.6117	4.6536	266.8519	0.9284	4.0831	10.1442	48.9635	11.7946	500.7960	1683.2691	17.0503	9.6157	300.5076	61.0157
42	378.4404	4.6976	377.6417	2.0448	4.6268	22.8964	42.0211	20.5372	2299.5981	583.6764	31.2304	26.7086	423.0301	133.7596
69	932.0872	4.4753	244.5168	1.4420	4.3106	10.9269	28.4866	21.9680	474.6807	1374.2380	22.4870	24.1908	285.4561	74.6866
51	1133.151	4.7965	234.5423	1.1178	4.5789	10.8088	61.8745	15.7831	271.7452	2687.6530	21.2742	18.9875	406.1639	76.5799
39	1143.375	4.6698	209.4606	0.9259	4.2335	8.6408	19.1859	11.5879	230.6507	2997.9420	12.4523	17.2647	225.3694	63.7339
36	696.5461	4.0935	230.7451	0.9888	3.7406	7.9863	15.6933	24.7861	296.7477	2414.1245	18.4363	11.0771	304.1955	63.2785

table cont'd

Site	P (mg/kg)	As (mg/kg)	Ba (mg/kg)	Be (mg/kg)	Cd (mg/kg)	Co (mg/kg)	Cr (mg/kg)	Cu (mg/kg)	Mn (mg/kg)	Na (mg/kg)	Ni (mg/kg)	Pb (mg/kg)	Si (mg/kg)	Zn (mg/kg)
59	873.1454	4.6342	303.2589	1.3828	4.4708	9.7369	46.5539	33.1097	260.3360	2574.6940	22.8290	22.5968	417.8994	70.4250
57	669.8324	3.6598	256.6855	1.2350	4.0064	9.4549	22.7103	14.8416	382.2937	1595.4973	21.3159	32.7794	249.2669	51.8787

Table D9. Subset of soil samples at the depth with HCl.

Site	P (mg/kg)	As (mg/kg)	Ba (mg/kg)	Be (mg/kg)	Cd (mg/kg)	Co (mg/kg)	Cr (mg/kg)	Cu (mg/kg)	Mn (mg/kg)	Na (mg/kg)	Ni (mg/kg)	Pb (mg/kg)	Si (mg/kg)	Zn (mg/kg)
23	713.6503	4.8799	189.6964	1.6118	4.7173	17.0983	90.6044	17.2584	464.5097	3212.2605	39.3244	58.5151	418.0347	105.7534
17	630.7339	4.8896	348.2310	2.5320	4.8289	17.5099	96.3495	26.7347	880.9684	653.7712	46.2081	70.9348	361.2690	123.5381
34	583.2895	4.5407	242.8993	1.4330	4.5723	10.0440	36.1840	10.6723	32.9920	3484.3000	26.1497	45.5317	433.2667	70.5897
61	598.8251	6.3642	290.0310	1.8067	5.9172	16.9281	67.4507	22.5725	444.1786	2225.5425	33.2478	95.6715	227.5468	123.0735
29	546.6667	3.6831	232.9789	2.1420	3.8239	13.6259	62.1253	21.0870	393.7426	2274.8460	39.0454	47.7187	477.1501	114.8877
19	575.3067	4.7398	352.4945	2.0409	4.5635	14.8201	64.2033	22.2691	441.8569	1258.7263	38.8778	65.1896	437.4502	99.1473
63	831.875	4.7354	153.4855	1.5920	4.4396	10.5905	27.0446	11.6630	357.3793	1153.3634	24.7778	46.8540	359.8107	63.4016
48	597.8261	5.7628	232.7837	1.2391	5.1625	21.6607	109.5751	23.7460	279.2260	1469.6180	31.8802	56.1723	383.0624	158.3349
42	706.3725	5.4771	540.8823	2.2437	5.1557	30.4594	210.2192	26.8537	1456.3488	710.9519	58.2484	68.7900	683.7081	189.1956
69	663.648	4.8551	264.3981	2.0421	4.7867	13.3532	53.9712	18.2985	132.4094	1867.3304	36.7296	57.2426	481.0183	93.9138
51	606.2706	3.8427	188.5751	1.7808	3.8789	13.4801	181.4088	16.7455	115.3771	3386.0638	111.8184	576.1110	302.7161	80.4260
39	636.4499	5.0002	282.9943	1.3709	4.3976	12.0498	45.4685	19.5652	316.5477	2547.8716	28.6629	60.0951	299.7761	109.1946
36	541.2141	4.5346	264.9100	1.5764	4.3275	9.8993	61.0254	16.7696	31.0602	1690.7675	29.0511	59.5323	215.8740	85.1812
59	467.8354	4.3914	140.9517	1.7892	4.5711	11.6329	46.0426	12.3099	132.1186	3538.3035	39.9464	35.8189	321.7664	79.9292
57	647.7077	4.8342	223.1345	1.7763	4.6843	11.8205	84.6800	13.0570	234.4979	2317.4205	34.2158	67.9666	516.2921	76.3356

Table D10. Years with mean ring width values, ring width indices from 1940-2018 and PC1 loadings for 1975-2018.

Year	Mean Ring Width (mm)	Ring Width Indices	PC1 Loadings
2018	1.1916	0.9464	0.80
2017	1.2787	1.0444	0.76
2016	1.3271	1.1307	0.82
2015	1.2785	1.1174	0.70

table cont’d

Year	Mean Ring Width (mm)	Ring Width Indices	PC1 Loadings
2014	1.0595	0.9506	0.77
2013	0.9893	0.929	0.64
2012	1.0153	0.959	0.75
2011	1.0048	0.8898	0.87
2010	0.8770	0.7973	0.69
2009	1.1928	1.055	0.80
2008	0.9164	0.8327	0.87
2007	1.0384	1.1086	0.80
2006	0.8651	0.8296	0.84
2005	1.3536	1.2738	0.84
2004	1.1957	1.0818	0.85
2003	1.3715	1.0781	0.86
2002	1.0312	0.721	0.84
2001	1.0427	0.7102	0.84
2000	0.9456	0.6612	0.90
1999	1.2875	0.8946	0.87
1998	1.2599	0.8459	0.80
1997	1.7679	1.0747	0.78
1996	1.5510	0.9365	0.74
1995	1.9337	1.1398	0.73
1994	2.0389	1.1187	0.77
1993	2.2928	1.2857	0.83
1992	2.0758	1.145	0.84
1991	2.5696	1.4847	0.76
1990	1.5049	0.8446	0.86
1989	1.4513	0.8242	0.85
1988	1.4343	0.8607	0.89
1987	1.3007	0.8027	0.86

table cont’d

Year	Mean Ring Width (mm)	Ring Width Indices	PC1 Loadings
1986	1.1521	0.7294	0.76
1985	1.1354	0.711	0.77
1984	1.4222	0.8518	0.78
1983	1.5271	0.9237	0.82
1982	1.5075	0.8913	0.80
1981	1.7639	1.003	0.81
1980	2.0609	1.1402	0.61
1979	1.8328	0.9924	0.66
1978	1.7604	0.9298	0.61
1977	2.0237	1.021	0.47
1976	2.0906	1.054	0.46
1975	2.7997	1.4316	0.52
1974	2.3982	1.1931	
1973	1.7044	0.8593	
1972	2.0858	1.0969	
1971	1.4704	0.7266	
1970	1.5953	0.7966	
1969	1.2626	0.6199	
1968	1.2087	0.7286	
1967	1.4864	0.9312	
1966	1.6927	0.996	
1965	1.6576	1.0394	
1964	1.8447	1.1389	
1963	1.6618	1.046	
1962	1.7461	1.1161	
1961	1.7113	1.1212	
1960	1.1986	0.8545	
1959	1.4165	0.9941	

table cont’d

Year	Mean Ring Width (mm)	Ring Width Indices	PC1 Loadings
1958	1.0832	0.7438	
1957	1.1301	0.791	
1956	1.0801	0.7578	
1955	1.1008	0.8271	
1954	1.3661	0.9187	
1953	1.6283	1.0409	
1952	1.8922	1.1097	
1951	1.5002	0.8978	
1950	1.5313	0.9311	
1949	2.0025	1.1703	
1948	1.7880	1.0242	
1947	1.7501	0.9652	
1946	1.9093	1.1035	
1945	1.9591	1.1471	
1944	1.6417	0.9969	
1943	1.4717	0.8892	
1942	1.4177	0.8886	
1941	1.2238	0.8597	
1940	1.4000	1.0241	

LITERATURE CITED

Allen JA, Pezeshki SR, Chambers JL. 1996. Interaction of flooding and salinity stress on baldcypress (*Taxidium distichum*). Tree Physiology 16:307-313.

Allen, S.T., Keim, R.F., Dean T.J. 2019. Contrasting effects of flooding on tree growth and stand density determine aboveground production, in baldcypress forests. Forest Ecology and Management 432:345-355.

Allen ST, Whitsell ML, Keim RF. 2015. Leaf area allometrics and morphometrics in baldcypress. Canadian Journal of Forest Research 45:963-969.

Andersen, J. 1976. An ignition method for determination of total phosphorus in lake sediments. Water Resources 10 (4): 329–331.

Baker DE, Amacher MC. 1983. Nickel, Copper, Zinc and Cadmium in Page AL, ed. Methods of Soil Analysis: Part 2 Checmical and Microbiological Properties, Wiley.

Bohora SB. 2012. Spatial variability in response of deltaic baldcypress forests to hydrology and climate. Louisiana State University.

Bunn AG, Graumlich LJ, Urban DL. 2005. Trends in twentieth-centruy tree growth at high elevations in the Sierra nevada and White Mountains, USA. The Holocene 15:481-488.

Chao X, Yafei J. 2020. Numberical modeling of flow, sediment, and salinity in Lake Pontchartrain during the Bonnet Carre Spillway flood release. Pages 144-154: World Environmental and Water Resources Congress.

Coastal Protection and Restoration Authority (CPRA) of Louisiana. 2020. Coastwide Reference Monitoring System-Wetlands Monitoring Data. Retrieved from Coastal Information Management System (CIMS) database. http://cim.coastal.louisiana.gov. Accessed 01/04/2020.

Conner WH, Ozalp M. 2002. Baldcypress restoration in a saltwater damaged area of South Carolina. Asheville, NC: U.S. Department of Agriculture, Forest Service, Southern Research Station. Report no.

Cook ER, Holmes RL. 1986. Guide for computer program ARSTAN. University of Arizona, Tuscon, AR.: Labratory of Tree-Ring Research.

Cook ER, Peters K. 1981. The smoothing slpline: A new approoach to standardizing forest interior tree-ring width series for dentrochimatic studies. Tree Ring Bulletin 41:45-53.

Day JW, et al. 2012. Ecological response of forested wetlands with and without large-scale Mississippi River input: Implications for management. Ecological Engineering 46:57-67.

Day JWJ, Hall CAS, Kemp WM, Yanez-Aranchiba A. 1989. Estuarine Ecology. John Wiley & Sons, Inc.

Day JWJ, Shaffer GP, Britsch LD, Reed DJ, Hawes SR, Cahoon D. 2000. Pattern and process of land loss in the Mississippi Delta: A spatial and temporal analysis of wetland habitat change. Estuarine Research Federation 23:425-438.

Day J., Lane R.R., Moerschbaecher M., DeLaune R, Mendelssohn I, Baustian J, Twilley R.R.. 2013. Vegetation and soil dynamics of a Louisiana estuary receiving pulsed Mississippi River water following Hurricane Katrina. Estuaries and Coasts 36:665-682.

Dean, TJ, Long JN. 1986. Variation in sapwood area-leaf area relations within two stands of lodgepole pine. Forest Science 32 (3): 749-758.

Dean TJ, Long JN, Smith FW. 1988. Bias in leaf area-sapwood area ratios and its impact on growth analysis in Pinus contorta. Trees: Structure and Function 2:104-109.

DeLaune RD, Devai I, Crozier CR, Kelle P. 2002. Sulfate reduction in Louisiana marsh soils of varying salinities. Communications in Soil Science and Plant Analysis 33:79-94.

Diamond, JS, Epstein JM, Cohen MJ, McLaughlin DL, Hsueh YH, Keim RF, Duberstein JA. In press. A little releif: Ecological functions and autogenesis of wetland microtopography.

Edwards BL, Allen ST, Braud DH, Keim RF. 2019. Stand density and carbon storage in cypress-tupelo wetland forests of the Mississippi River delta. Forest Ecology and Management 441:106-114.

Fritts, HC. 1976. Tree Rings and Climate. Academic Press. London.

Grosenbaugh LR. 1952. Shortcuts for cruisers and scalers in Agriculture USDo, ed. New Orleans, LA: U.S. Forest Service, Southern Forest Experiment Station.

Hackney CT, Avery GB. 2015. Tidal wetland community response to varying Levels of flooding by saline water. Wetlands 35:227-236.

Hiatt M, Snedden G, Day JW, Rohli RV, Nyman JA, Lane R, Sharp LA. 2019. Drivers and imparts of water level fluctuations in the Mississippi River delta: Implications for delta restoration. Estuarine, Coastal and shelf Science 224:117-137.

Hill KD, Dauphinee TM, Woods DJ. 1986. The extension of the practical salinity scale 1978 to low salinites. IEEE Journal of Oceanic Engineering, 11 (1): 109-112.

Hillmann E, Butcher K, Barrett S, Krolopp E, Lemon MG, Lopez J. 2020. Swamp restoration in the Pontchartrain Basin: Update January 2010-August 2019. The Lake Pontchartrain Basin Foundation.

Hoogsteen MJJ, Lantinga EA, Bakker EJ, Groot JCJ, Tittonell PA. 2015. Estimating soil organic carbon through loss on ignition: effects of ignition conditions and structural water loss. European Journal of Soil Science 66:320-328.

Howard PJA, Howard DM. 1990. Use of organic carbon and loss-on-ignition to estimate soil organic matter in different soil types and horizons. Biology and Fertility of Soils:306-310.

Hsueh Y, Chambers JL, Krauss KW, Allen ST, Keim RF. 2016. Hydrologic exchanges and baldcypress water use on deltaic hummocks, Louisiana, USA. Ecohydrology 9:1452-1463.

Hunter R, Day J, Shaffer GP, Lane RR, Englande A, Reimers R, Kandalepas D, Wood WB, Day J, Hillmann E. 2016. Restoration and Management of a Degraded Baldcypress Swamp and Freshwater Marsh in Coastal Louisiana. Water 8.

Keddy PA, Campbell D, McFalls T, Shaffer GP, Moreau R, Dranguet C, Heleniak R. 2007. The wetlands of Lakes Pontchartrain and Maurepas: Past, present and future. Environmental Reviews 15:43-77.

Keim RF, Dean TJ, Chambers JL, Conner WH. 2010. Stand density relationships in bald Cypress. Forest Science 56:336-343.

Keim RF, Amos JB. 2012. Dendrochronological analysis of baldcypress (Taxodium distichum) responses to climate and contrasting flood regimes. Canadian Journal of Forest Research 42:423-436.

Keim RF, Dean TJ, Chambers JL. 2013a. Flooding effects on stand development in cypress-tupelo. 15th Biennial Southern Silivicultural Research Conference. Hot Springs, Arkansas: USDA Forest Service General Technical Report SRS-XX.

Keim RF, Zoller JA, Braud DH, Edwards BL. 2013b. Classification of forested wetland degradation using ordination of multitemporal reflectance. Wetlands 33:1103-1115.

Kirwan ML, Temmerman S, Skeehan EE, Guntenspergen GR, Fagherazzi S. 2016. Overestimation of marsh vulnerability to sea level rise. Nature Climate Change 6:253-260.

Krairapanond N, DeLaune RD, Patrick WHJ. 1991. Seasonal Distribution of Sulfur Fractions in Louisiana Salt marsh Soils. Estuaries 14:17-28.

Krauss KW, Duberstein JA, Doyle TW, Conner WH, Day RH, Inabinette LW, Whitbeck JL. 2009. Site condition, structure, and growth of baldcypress along tidal/non-tidal salinity gradients. Wetlands 29:505-519.

Lewis EL, Perkin RG. 1978. Salinity: Its definition and calculation. Journal of Geophysical Research 83 (C1): 466-478.

Lickey EB, Walker GL. 2002. Population genetic structure of baldcypress (Taxodium Distichum [L.] Rich. Var. Distichum) and pondcypress (T. Distichum Var. Imbricarium [Nuttall] Croom): Biogeographic and Taxonomic Implications. Southeastern Naturalist 1:131-148.

Liu X, Conner WH, Song B, Jayakaran AD. 2017. Forest composition and growth in a freshwater forested wetland community across a salinity gradient in South Carolina, USA. Forest Ecology and Management 389:211-219.

McAlhaney, A. 2018. Baldcypress and black willow growth response to contrasting flood regimes, climate and competition in the Atchafalaya River Basin, Louisiana, Renewable Natural Resources, Louisiana State University.

McAlhaney A, Keim RF, Allen ST. In press. Comparison of individual-tree competition metrics in an undeven-aged, baldcypress (*Taxodium distichum*) and blackwillow (*Salix nigra*) floodplain forest.

McDaniel. 1990. Soil survey of Tangipahoa Parish, Louisiana. Soil Conservation Services, United States Department of Agriculture.

Mehlich A. 1984. Mechlich-3 Soil Test Extractant- A Modification of Mechlich-2 Extractant. Communications in Soil Science and Plant Analysis 15:1409-1416.

Myers RS, Shaffer GP, Llewellyn DW. 1995. Bald Cypress (Taxidium Distichum (L.) Rich.) Restoration in Southeastern Louisiana-the relative effects of herbivory, flooding, competition and machronutrients. The Society of Wetlands Scientists 15:141-148.

Nyman JA, Walters RJ, Delaune RD, Patrick WH. 2006. Marsh vertical accretion via vegetative growth. Estuarine, Coastal and Shelf Science 69:370-380.

O'Hara KL. 1988. Stand structure and growing space efficiency following thinning in an even-aged Douglas-fir stand. Canadian Journal of Forest Research 18:859-866.

Powell AS, Jackson L, Ardón M. 2016. Disentangling the effects of drought, salinity, and sulfate on baldcypress growth in a coastal plain restored wetland. Restoration Ecology 24:548-557.

Prietzel J, Cronauer H, Strehl C. 1996. Determination of dissolved total sulfur in aqueous extracts and seepage water of forest soils. International Journal of Environmental Anylitical Chemistry 64:193-203.

Reddy KR, DeLaune RD. 2008. Biogeochemistry of Wetlands: Science and Applications. Boca Raton, Florida: CRC Press Taylor & Francis Group.

Reineke LH. 1993. Perfecting a stand-density index for even-aged forests. Journal of Agricultural Research 46:627-638.

Shaffer GP, Day J, Kandalepas D, Wood WB, Hunter R, Lane RR, Hillmann E. 2016. Decline of the Maurepas Swamp, Pontchartrain Basin, Louisiana, and approaches to restoration. Water 8.

Shaffer GP, et al. 2009. The MRGO Navigation Project: A massive human-induced environmental, economic, and storm disaster. Journal of Coastal Research 10054:206-224.

Shaffer GP, Wood WB, Hoeppner SS, Perkins TE, Zoller J, Kandalepas D. 2009. Degradation of baldcypress–water tupelo swamp to marsh and open water in Southeastern Louisiana, U.S.A.: An Irreversible Trajectory? Journal of Coastal Research 10054:152-165.

Speer JH. 2012. Fundamentals of Tree Ring Research.

Spratt HGJ, Morgan MD. 1990. Sulfur cycling in a cedar- dominated, freshwate wetland. Limnology and Oceanography 35:1586-1593.

Stahle DW, Edmondson JR, Howard IM, Robbins CR, Griffin RD, Carl A, Hall CB, Stahle DK, Torbenson MCA. 2019. Longevity, climate sensitivity, and conservation status of wetland trees at Black River, North Carolina. Environmental Research Communications 1.

Thomas BL, Doyle T, Krauss K. 2015. Annual Growth Patterns of Baldcypress (Taxodium distichum) Along Salinity Gradients. Wetlands 35:831-839.

Vertessy RA, Benyon RG, O'Sullivan PR, Gribben PR. 1995. Relationships between stem diameter, sapwood area, leaf area and transpiration in young mountian ash forest. Tree Physiology 15:559-567.

Wang H, Krauss KW, Noe GB, Stagg CL, Swarzenski CM, Duberstein JA, Conner WH, DeAngelis DL. 2020. Modeling soil porewater salinity response to drought in tidal freshwater forested wetlands. Journal of Geophysical Research: Biogeosciences 125.

Waring RH. 1983. Estimating forest growth and efficniecy in relation to canopy leaf area. Pages 327-354 in MacFadyen A, Ford ED, eds. Advances in Ecological Research. London, UK: Academic Press.

Waring RH, Newman K, Bell J. 1981. Efficiency of tree crowns and stemwood production at different canopy leaf densities. Foresty 54:15-23.

Wigley TML, Briffa KR, Jones PD. 1984. On the average value of correlated time series, with applications in dendroclimatology and hydrometeorology. American Meteorological Society 23:201-213.

Willis JM, Gambrell RP, Hester MW. 2011. Mercury concentrations in oligohaline wetland vegetation and associated soil biogeochemistry. Environ Monit Assess 181:373-383.

U.S. Army Corps of Engineers, Mississippi River Gulf Outlet (MRGO) Ecosystem Restoration Plan Final Feasibility Report, New Orleans District 7400 Lake Avenue New Orleans, Louisiana 70118, (2012).

U.S.D.A. Natural Resources Conservation Service: Wetland Obligate Species webpage, accessed November 20, 2018, https://plants.usda.gov/core/profile?symbol=TADI2

U.S. EPA, 1993. Methods for Determination of Inorganic Substances in Environmental Samples. EPA/600/R-93/100 (Washington D.C).

VITA

Stephanie M. Moothart is a native of Fort Collins, Colorado. She received her Bachelor of Science in Ecosystem Science and Sustainability and her Bachelor of Art in Sociology with an Environmental Concentration at Colorado State University in 2016. After graduation, she worked as a Forestry Technician for Colorado Parks and Wildlife for two years gaining a passion for forest research. Following that, she continued her education in the School of Renewable Natural Resources at Louisiana State University working towards her Masters of Science degree with a concentration in watershed science. She worked under the guidance of Dr. Richard Keim in the Forest and Wetland Ecohydrology Lab studying cypress growth in response to marine influence and stand density. She plans to begin her career working in the natural resource field in Oregon.